Journal of Visualized Experiments

Defining Gene Functions in Tumorigenesis by Ex Vivo Ablation of Floxed Alleles in Malignant Peripheral Nerve Sheath Tumor Cells

--Manuscript Draft--

Article Type:	Invited Methods Article - JoVE Produced Video
Manuscript Number:	JoVE62740R1
Full Title:	Defining Gene Functions in Tumorigenesis by Ex Vivo Ablation of Floxed Alleles in Malignant Peripheral Nerve Sheath Tumor Cells
Corresponding Author:	Jody Fromm Longo Medical University of South Carolina Charleston, SC UNITED STATES
Corresponding Author's Institution:	Medical University of South Carolina
Corresponding Author E-Mail:	jodylongo@gmail.com
Order of Authors:	Jody Fromm Longo
	Stephanie Brosius
	Steven Carroll
Additional Information:	
Question	**Response**
Please specify the section of the submitted manuscript.	Cancer Research
Please indicate whether this article will be Standard Access or Open Access.	Standard Access ($1400)
Please indicate the **city, state/province, and country** where this article will be **filmed**. Please do not use abbreviations.	Charleston, SC, USA
Please confirm that you have read and agree to the terms and conditions of the author license agreement that applies below:	I agree to the Author License Agreement
Please provide any comments to the journal here.	

TITLE:

Defining Gene Functions in Tumorigenesis by *Ex Vivo* Ablation of Floxed Alleles in Malignant Peripheral Nerve Sheath Tumor Cells

AUTHORS AND AFFILIATIONS:

Jody Fromm Longo[1], Stephanie N. Brosius[2,3], Steven L. Carroll[1]

[1]Department of Pathology and Laboratory Medicine, Medical University of South Carolina, Charleston, SC 29425, USA

[2]Department of Pathology, University of Alabama at Birmingham, Birmingham, AL 35294-0017, USA

[3]Medical Scientist Training Program, University of Alabama at Birmingham, Birmingham, AL 35294-0017, USA

Email addresses of co-authors:

Jody Fromm Longo (longoj@musc.edu)

Stephanie N. Brosius (stephanie.brosius@gmail.com)

Corresponding author:

Steven L. Carroll (carrolst@musc.edu)

KEYWORDS:

Genetically modified mice; sarcoma; Cre-expressing adenovirus; flow cytometry; survival assays; proliferation assays; xenografting; RNA-Seq; embryonic lethal knockout.

SUMMARY:

Here, we present a protocol for performing gene knockouts that are embryonic lethal *in vivo* in genetically engineered mouse model-derived tumors and then assessing the effect that the knockout has on tumor growth, proliferation, survival, migration, invasion, and the transcriptome *in vitro* and *in vivo*.

ABSTRACT:

The development of new drugs that precisely target key proteins in human cancers is fundamentally altering cancer therapeutics. However, before these drugs can be used, their target proteins must be validated as therapeutic targets in specific cancer types. This validation is often performed by knocking out the gene encoding the candidate therapeutic target in a genetically engineered mouse (GEM) model of cancer and determining what effect this has on tumor growth. Unfortunately, technical issues such as embryonic lethality in conventional knockouts and mosaicism in conditional knockouts often limit this approach. To overcome these limitations, an approach to ablating a floxed embryonic lethal gene of interest in short-term cultures of malignant peripheral nerve sheath tumors (MPNSTs) generated in a GEM model was developed**.**

This paper describes how to establish a mouse model with the appropriate genotype, derive

short-term tumor cultures from these animals, and then ablate the floxed embryonic lethal gene using an adenoviral vector that expresses Cre recombinase and enhanced green fluorescent protein (eGFP). Purification of cells transduced with adenovirus using fluorescence-activated cell sorting (FACS) and the quantification of the effects that gene ablation exerts on cellular proliferation, viability, the transcriptome, and orthotopic allograft growth is then detailed. These methodologies provide an effective and generalizable approach to identifying and validating therapeutic targets *in vitro* and *in vivo.* These approaches also provide a renewable source of low-passage tumor-derived cells with reduced *in vitro* growth artifacts. This allows the biological role of the targeted gene to be studied in diverse biologic processes such as migration, invasion, metastasis, and intercellular communication mediated by the secretome.

INTRODUCTION:

Before the last two decades, the treatment of human cancers relied heavily on radiotherapy and chemotherapeutic agents that broadly targeted rapidly proliferating cellular populations by damaging DNA or inhibiting DNA synthesis. Although these approaches did inhibit cancer cell growth, they also had deleterious side effects on normal rapidly proliferating cell types such as intestinal epithelial cells and hair follicle cells. More recently, cancer therapy has begun to utilize chemotherapeutic agents that precisely target proteins within signaling pathways that are critically important for the growth of an individual patient's neoplasm. This approach, commonly referred to as "Precision Medicine," has led to the development of an ever-expanding repertoire of monoclonal antibodies and small molecular inhibitors. These agents effectively inhibit tumor cell proliferation and survival while avoiding the deleterious side effects on normal cell types seen with conventional chemotherapeutic agents and radiotherapy. Monoclonal antibodies used for the treatment of human cancers most commonly target cell surface molecules such as growth factor receptors[1] (e.g., the large family of membrane-spanning receptor tyrosine kinases) and immune response modulators[2] (e.g., programmed cell death protein 1, programmed death-ligand 1). Small molecular inhibitors can inhibit either cell surface proteins or signaling proteins that are located intracellularly[3]. However, to effectively employ these new therapeutic agents, it must be established that a particular cancer is dependent upon the molecule that is being targeted by a candidate therapeutic agent.

Although these new therapeutic agents have more focused effects, many of them still inhibit the action of more than one protein. In addition, multiple agents with varying effectiveness and specificity are often available to target a specific protein. Consequently, during preclinical investigations, it is wise to use additional approaches such as genetic ablation to validate a candidate protein as a therapeutic target. One especially useful approach to validating a protein as a therapeutic target is to ablate the gene encoding the candidate protein in a genetically engineered animal model that develops the specific cancer type of interest. This approach can be relatively straightforward if mice with a null mutation (either a natural mutation, a genetically engineered null mutation (a "knockout"), or a null mutation introduced by a gene trap] are available, and the mice are viable into adulthood. Unfortunately, mice with a null mutation that meet these criteria are often not available, typically because the null mutation results in death embryonically or in the first days of postnatal life. In this circumstance, mice prone to develop the tumor type of interest may instead be crossed to mice in which key segments of the gene of

interest are flanked by loxP sites ("floxed"), which allows the gene to be ablated by introducing a transgene expressing Cre recombinase into the tumor cells (a conditional knockout). This approach provides several advantages. First, if a Cre driver is available that is expressed in the tumor but not in the cell type that led to death in conventional knockouts, this approach can potentially validate the candidate therapeutic target. Second, ablating the gene encoding the candidate protein in tumor cells but not in other intratumoral elements such as tumor-associated fibroblasts or immune cells allows the investigator to distinguish between cell-autonomous and non-cell-autonomous effects of the therapeutic target. Finally, a tamoxifen-inducible Cre driver ($CreER^{T2}$) allows the investigator to delete the gene of interest at different stages in tumor development and define the window in which the candidate therapeutic agent is most likely to be effective.

Unfortunately, there are also technical issues that can limit the use of conditional knockouts in tumors arising in GEM models. For instance, a Cre driver that is expressed in tumor cells and avoids gene deletion in normal cells essential for life may not be available. Another issue, which may be underestimated, is that Cre and $CreER^{T2}$ drivers often variably ablate floxed alleles in mice, resulting in mosaicism for the null mutation in a GEM cancer. When this occurs, tumor cells in which the targeted gene has not been ablated will continue to proliferate rapidly, overgrowing the tumor cells with ablated alleles. Mosaicism in Cre driver lines can occur due to non-ubiquitous Cre expression in the lineage targeted and by failed recombination in individual cells independent of Cre expression[4]. This is a known phenomenon of Cre drivers that is cell-type dependent and should be considered during experimental design and data interpretation. Mosaicism can mask the effect of the knockout and lead an investigator to erroneously conclude that the gene of interest is not essential for tumor cell proliferation and/or survival and thus is not a valid therapeutic target.

Several of these problems were encountered in a previous study that attempted to determine whether the receptor tyrosine kinase erbB4 was a potential therapeutic target in MPNST cells[5]. In these studies, mice were used that express a transgene encoding the neuregulin-1 (NRG1) isoform glial growth factor-β3 (GGFβ3) under the control of the Schwann cell-specific myelin protein zero promoter (P_0-GGFβ3 mice). P_0-GGFβ3 mice develop multiple plexiform neurofibromas that progress to become MPNSTs via a process that recapitulates the processes of neurofibroma pathogenesis and plexiform neurofibroma-MPNST progression seen in patients with the autosomal dominant tumor susceptibility syndrome neurofibromatosis type 1 (NF1)[6]. When crossed to mice with a *Trp53* null mutation, the resulting P_0-GGFβ3;$Trp53^{+/-}$ mice develop MPNSTs *de novo* as is seen in *cis*-$Nf1^{+/-}$;$Trp53^{+/-}$ mice.

These MPNSTs recapitulate the progression from World Health Organization (WHO) grade II to WHO grade IV lesions seen in humans[7]. In P_0-GGFβ3 mice, MPNSTs arise within pre-existing plexiform neurofibromas in the trigeminal nerve (58%) and spinal dorsal nerve roots (68%)[7]; the MPNSTs arising in P_0-GGFβ3;$Trp53^{+/-}$ mice have a highly similar distribution. In humans, MPNSTs most commonly arise in the sciatic nerve followed by the brachial plexus, spinal nerve roots, vagus, femoral, median, sacral plexus, popliteal obturator, and posterior tibial and ulnar nerves[8]. This tumor distribution in these GEM models is somewhat different from what is seen in humans.

However, the MPNSTs that arise in P_0-GGFβ3 and P_0-GGFβ3;*Trp53*$^{+/-}$ mice are histologically identical to human MPNSTs, carry many of the same mutations seen in human MPNSTs, and recapitulate the process of neurofibroma-MPNST progression seen in NF1 patients. The generation of P_0-GGFβ3 or P_0-GGFβ3;*Trp53*$^{+/-}$ mice that were *Erbb4*$^{-/-}$ was not feasible as mice with two *Erbb4* null alleles die *in utero* at embryonic day 10.5 secondary to cardiac defects[9]. Because rescuing *Erbb4* expression in the heart by introducing a cardiac-specific *Erbb4* transgene (α-myosin heavy chain (MHC)-*Erbb4*) results in viable *Erbb4*$^{-/-}$ mice[10], the generation of mice with a complicated P_0-GGFβ3;*Trp53*$^{+/-}$;α-MHC-*Erbb4*;*Erbb4*$^{-/-}$ genotype was attempted.

However, the matings did not produce mice in the expected Mendelian ratios, indicating that the desired genotype was deleterious. Therefore, the generation of P_0-GGFβ3;*Trp53*$^{+/-}$ mice with floxed *Erbb4* alleles[11] and a CreER^{T2} driver was attempted to allow the deletion of *Erbb4* in the MPNSTs arising in these mice. In these animals, numerous tumor cells with intact *Erbb4* alleles were still present (mosaicism). The mosaicism observed could result from inefficient tamoxifen delivery, which resulted in differences in recombination efficiency within the tissue. The possibility of spontaneous compensatory mechanisms could further contribute to mosaicism in tamoxifen-mediated recombination by bypassing the requirement for *Erbb4* expression. It is feasible that the loss of *Trp53* makes tumor cells susceptible to additional spontaneous "permissive" mutations that could confuse the interpretation of the data. As it seemed likely that the *Erbb4*-intact MPNST cells would mask the consequences of ablating *Erbb4* in other tumor cells, this approach was abandoned.

These obstacles led to the development of a methodology for ablating *Erbb4* in very early passage MPNST cells using an adenovirus expressing Cre recombinase and eGFP. These cells can be separated from non-infected cells using FACS, which markedly reduces mosaicism for the ablated *Erbb4* gene. Below, the methods used to achieve this, together with the methods used to assess the effects of gene ablation *in vitro* and *in vivo*, are described. The following protocol is an example of how to produce tumor-bearing mice that yield tumors carrying floxed alleles of embryonic lethal genes of interest for *ex vivo* excision prior to *in vivo* allograft tumor growth assessment. This includes a description of the approaches used to analyze the effect that *Erbb4* ablation exerts on tumor cell proliferation, survival, and gene expression *in vitro* and proliferation, survival, and angiogenesis in orthotopic allografts.

PROTOCOL:

Prior to performing any procedures with mice, all procedures must be reviewed and approved by the Institutional Animal Care and Use Committee. The protocol described in this manuscript was approved by the Institutional Animal Care and Use Committee of the Medical University of South Carolina. This protocol was performed by properly trained personnel following MUSC's institutional animal care guidelines.

1. **Generation of mice that develop MPNSTs homozygous for *Erbb4*^{flox} alleles**

1.1. Produce the F1 generation of P_0-GGFβ3;*Trp53*$^{+/-}$;*Erbb4*$^{fl/+}$ animals by mating P_0-

GGFβ3;*Trp53*$^{+/-}$ mice[7] with *Erbb4*$^{fl/fl}$ mice[11]. Use a Punnet square (**Figure 1**) to guide the breeding scheme to ensure that enough male and female F1 pups are generated with the desired P_0-GGFβ3;*Trp53*$^{+/-}$;*Erbb4*$^{fl/+}$ genotype.

1.2. Genotype F1 offspring by isolating genomic DNA from a tail snip and then perform PCR using previously described primers to detect the P_0-GGFβ3 transgene[12], *Trp53* wild type (+) and null (-) alleles[7], and *Erbb4*^{flox} and *Erbb4* wild-type alleles[13].

1.2.1. Isolate tail DNA using methods detailed on jacks-lab.mit.edu/protocols.

1.2.2. Make the PCR reaction mix with 25 ng DNA, 0.25 nM dNTPs, 0.02 U/µL Taq, 0.5 µM of each primer, and 1x PCR buffer. Perform PCR reaction with a single 95 °C incubation (to melt the genomic DNA and activate Taq) for 1 min followed by 35 PCR cycles of 94 °C, 10 s (melting); 55 °C, 30 s (annealing); 72 °C, 40 s (extension) followed by a single 72 °C (extension) for 5 min. Store the reactions at 4 °C until ready to run on a 1.2–1.5% agarose gel.

NOTE: Annealing temperature depends on the PCR buffer system used; performing an annealing temperature gradient to determine the proper annealing temperature is recommended.

1.3. Produce the F2 generation of P_0-GGFβ3;*Trp53*$^{+/-}$;*Erbb4*$^{fl/fl}$ animals by mating the appropriate F1 progeny (P_0-GGFβ3;*Trp53*$^{-/+}$;*Erbb4*$^{fl/+}$) with each other.

NOTE: **Figure 1** illustrates the Punnet square predictions used to calculate the expected number of F2 offspring with the desired genotype.

1.4. Identify the animals with the desired P_0-GGFβ3;*Trp53*$^{-/+}$;*Erbb4*$^{fl/fl}$ genotype as described in step 1.2.

1.5. Mate F2 progeny to each other to maintain the P_0-GGFβ3;*Trp53*$^{-/+}$;*Erbb4*$^{fl/fl}$ colony and genotype all the pups. Confirm that the newly introduced floxed allele does not compromise survival or tumor latency. Achieve this by establishing cohorts (20 mice/cohort) of P_0-GGFβ3;*Trp53*$^{+/-}$ and P_0-GGFβ3;*Trp53*$^{+/-}$;*Erbb4*$^{fl/fl}$ mice and follow their survival and frequency of tumor occurrence.

1.6. Monitor animals several times per week until the experimental endpoint is reached (maximum allowable tumor size/humane endpoint approved by IACUC).

1.6.1. During the weekly monitoring, assess body weight, normal social and grooming behavior, and tumor size measurements. Arrange for veterinary assessment in case of weight loss of >10% of body weight, social seclusion, and hunching.

1.6.2. When a tumor-bearing mouse is identified and has reached its humane endpoint, humanely euthanize the animal using carbon dioxide inhalation followed by cervical dislocation and sterilely remove the tumor using a scalpel knife. Take tumor measurements by measuring

length, width, and depth using a caliper and weight tumor (mass and volume). Work quickly to avoid autolysis.

1.7. Section the tumor into three sections using breadloaf style cuts with a scalpel knife under sterile conditions to generate tissue segments for formalin fixation/paraffin-embedding (FFPE), early passage culture generation, and flash-frozen material (**Figure 2A**).

1.7.1. Ensure that Section 1 is approximately 10% of the total tumor volume, Section 2 is 70% of the total tumor volume, and Section 3 is 20% of the total tumor volume.

1.7.2. Take a portion of the tumor for the preparation of early passage cultures (see below).

1.7.3. Flash-freeze another portion for analytical analyses (e.g., immunoblots to verify that protein encoded by the targeted floxed gene is appropriately expressed).

1.7.4. Fix the remainder of the tumor in 4% paraformaldehyde overnight at 4 °C and then embed in paraffin (formalin-fixed paraffin-embedded (FFPE)) for diagnostic workup.

1.8. Stain 5 µm-thick FFPE tissue sections with hematoxylin and eosin (H&E) to confirm the tumor diagnosis by a qualified pathologist. If appropriate, perform immunohistochemical staining (IHC) to confirm the tumor diagnosis.

1.8.1. Immunostain MPNSTs for S100 calcium-binding protein B (S100β), nestin, and sex-determining region Y (SRY)-Box transcription factor 10 (Sox10)—three markers that are expressed in both MPNSTs and Schwann cells (tumor cell origin)[5,6,14,15]. Stain the tumors with antibodies recognizing erbB4, the protein encoded by the gene targeted for ablation in downstream steps.

1.8.2. To confirm the diagnosis, have a qualified veterinary or human pathologist assess all stained tumor slides following WHO diagnostic and grading criteria[5-7,16].

2. *Ex vivo* ablation of floxed *Erbb4* alleles in MPNST cells

2.1. Establish early passage cultures from freshly collected MPNST tissue by placing the tissue in 10 mL of ice-cold sterile phosphate-buffered saline (PBS) on ice and then transferring it to a sterile work area (**Figure 2B**)[16].

NOTE: All subsequent procedures are to be performed in a sterile tissue culture hood.

2.2. Mince the tumor tissue into 2–4 mm pieces and triturate 8–10 times in a 10 cm^2 treated tissue culture dish with 10 mL of growth medium. Culture these preparations in high glucose DMEM-10 growth medium (Dulbecco's modified Eagle's medium (DMEM) containing 10% fetal calf serum, 1% glutamine, 10 µg/mL streptomycin, and 10 IU/mL penicillin) supplemented with 10 nM neuregulin-1β (NRG1β) and 2 µM forskolin. Remember to add forskolin at this stage to

inhibit the growth of common contaminating cell types such as fibroblasts.

2.3. Maintain the mechanically dissociated tissue and cells for up to 3 days at 37 °C in a 5% CO_2 atmosphere to establish an early passage culture. Do not separate dispersed cells and remaining tissue fragments at this point.

2.4. Refresh the cultures with new medium every 3–4 days. Allow the tumor cells to proliferate until they are confluent.

2.5. Expand the early passage cultures by splitting the confluent cultures into several dishes. Remove the growth medium and wash cells with 1x dPBS. Then, add 1 mL of 0.25% trypsin for 2–5 min at room temperature per 10 cm^2 treated cell culture dish. Gently triturate the culture to facilitate detachment and generate a single-cell suspension.

2.5.1. Terminate the trypsinization by adding 2 mL of DMEM-10 growth medium. Collect the trypsinized cell mixture and transfer it to a 5 mL sterile centrifuge tube. Pellet the cells by centrifugation for 5 min at 500 × *g* at room temperature.

2.5.2. Resuspend the cell pellet in 5 mL of DMEM-10. Split the cells into two to four 10 cm cell culture dishes, each containing 10 mL of growth media (approximately 1×10^6 cells per dish).

2.6. After 5 passages (repeating steps in 2.5), use growth medium without NRG1β and forskolin. Immunostain a sample of the culture with an anti-S100β antibody to verify that the culture is composed solely of tumor cells. Maintain the cells in DMEM-10 growth medium in all subsequent passages.

2.7. At the next passage, count the cells and freeze down a portion of P_0-GGFβ3;*Trp53*$^{+/-}$;*Erbb4*$^{fl/fl}$ MPNST cells collected from confluent cultures (3×10^6 cells/vial).

2.8. Plate P_0-GGFβ3;*Trp53*$^{+/-}$;*Erbb4*$^{fl/fl}$ early passage MPNST cells at a density of 1.5×10^6 cells per 10 cm treated cell culture dish in DMEM-10 growth medium.

2.9. **Day 0:** (Approximately 12–16 h after plating), wash the adherent cultures with 2–4 mL of dPBS and infect with Ad5CMV-Cre/eGFP or Ad5CMV-eGFP at approximately 400 plaque-forming units (pfu)/cell in 10 mL of serum-free DMEM (i.e., 30 µL of 2×10^{10} pfu of virus per 10 cm dish). Ablate the floxed *Erbb4* alleles using the adenovirus at the maximum tolerated virus concentration (multiplicity of infection, MOI), as determined empirically. Refer to **Figure 2C** for a schematic of the workflow for this ablation.

2.10. **Day 1:** Approximately 16 h later, rescue the cultures by adding 10 mL of DMEM-10 to the infection cocktail.

2.11. **Day 2–3:** FACS sort infected cells following the recommended protocol from the core facility to sort eGFP-positive cells approximately 48 h after infection. Prior to FACS sorting, briefly

check cells for eGFP signal on a fluorescence microscope to ensure that the cultures have been efficiently infected (~50–100% positive cells). Return cells recovered after FACS to 10 cm tissue culture dishes; reserve one dish for genomic DNA isolation.

2.12. **Day 4–5:** After FACS sorting, let the cells recover in a tissue culture incubator for at least 24–48 h and then prepare the cells for *in vitro* cell-based analyses or *in vivo* grafting. Confirm *Erbb4* deletion via PCR using genomic DNA isolated from a portion of the sorted eGFP-positive cells. Verify that eGFP-positive cells are *ErbB4*-negative by PCR or by immunostaining a sample of the culture with an anti-erbB4 antibody.

2.12.1. Isolate genomic DNA from the cells using standard acid-guanidinium-phenol and chloroform-based DNA isolation method[17].

2.12.2. Perform standard PCR to distinguish floxed *Erbb4* alleles and ablated *Erbb4* alleles. Perform 40 cycles with 2 ng DNA, 20 µM primers 1 + 2 to produce a 250 bp *Erbb4*-null product and a 350 bp floxed product[13]. Perform both PCR and antibody-based approaches to confirm knockout when no reliable antibodies are available.

NOTE: Cells are ready for *in vitro* cell-based assays as described below. Many types of downstream analyses can be performed with cells prepared in this manner. The purpose of the protocols presented below is to provide a few examples of *in vitro* and *in vivo* applications of these tumor cells post-ablation of the *Erbb4* gene.

3. Proliferation and viability assays in MPNST cells with ablated *Erbb4* alleles

3.1. Perform proliferation assays over the next seven days on sorted MPNST cells plated in a multiwell plate using an image-based automated cytometer.

3.1.1. **Day 6:** Plate 2,000 cells per well in a final volume of 150 µL (~13,300 cells/mL) of growth medium in a 96-well plate. Perform measurements in triplicate for each experimental cohort and 4 daily endpoint reads (3 replicates x 2 conditions x 4 days).

3.1.2. **Days 7, 9, 11, 13:** Stain cells with Hoechst and propidium iodide (PI) dyes and image them on an automated plate reader to count the number of live and dead cells in each well. To achieve this, simultaneously stain the cells with Hoechst dye to stain the nuclei of both living and dead cells and with propidium iodide (PI) to label the dead cells. Perform all reads at the same time every day or every other day.

3.1.2.1. Add 50 µL of a 4x PI/Hoechst staining solution (4 µg/mL each) to each well quantified that day (e.g., Day 7 only), and incubate for 30 min at 37 °C in the tissue culture incubator. Keep the plate protected from light.

NOTE: The staining concentration of Hoechst needs to be empirically determined and can range from 1 to 10 µg/mL depending on the cell type.

3.1.2.2. Read the stained wells after incubation using the appropriate fluorescent channel on the automated cell imager. After reading, return the plate to the incubator for future reads on subsequent days (i.e., Days 9, 11, 13).

3.1.2.3. Quantify the staining intensities based on the imaging system used and calculate the number of dead cells, living cells, and total cells using the following settings: blue channel (377/50 nm, Hoechst): total cells (live and dead); red channel (531/40 nm, PI): dead cells only; blue – red (total – dead) = live cells.

3.2. Perform the cell viability assay over three days, if desired, following the assay manufacturers' protocol.

NOTE: Viability assays can be combined with proliferation assays by performing a triple stain including calcein AM (488/32 nm; green channel, specifically labels living cells), PI, and Hoechst. An apoptosis assay may also be performed using cultures set up as described above; the specific protocol will depend on the imaging system.

3.2.1. **Day 6:** Plate 4,000 cells per well in a final volume of 150 µL in a 96-well plate in triplicate.

3.2.2. **Days 7–9:** Add 2,000x bioluminescent cell viability assay reagents (see the **Table of Materials**), return the plate to the incubator, and read the plate 1 h later. Perform subsequent reads at the same time every day. For the bioluminescence (MTT) assays, perform the assay exactly as outlined in the manufacturer's instructions every 24 h for 72 h using a luminometer plate reader.

4. RNA-Seq analyses and identification of genes whose expression is altered by *Erbb4* loss

4.1. **Day 6:** Isolate total RNA from sorted MPNST cells using standard acid-guanidinium-phenol and chloroform-based methods. For experiments designed to detect changes in mRNA levels between two cohorts, prepare total RNA from at least three biological replicates in each cohort.

4.1.1. To eliminate events caused by the adenoviral vector or eGFP expression rather than *Erbb4* loss, isolate RNA from three biological replicates of P_0-GGFβ3;*Trp53*$^{+/-}$;*Erbb4*$^{fl/fl}$ MPNST cells transduced with Ad5CMV-Cre/eGFP and three biological replicates transduced with Ad5CMV-eGFP.

NOTE: Isolated RNA must have an RNA integrity number (RIN) score ≥ 8 for RNA-Seq analysis. Ensure that the sequencing core determines the RIN of all samples prior to constructing libraries.

4.2. Use 100–200 ng of high-quality total RNA from each sample to prepare RNA-Seq libraries (work with the core sequencing facility for this step). Perform high-throughput sequencing using a next-generation DNA sequencer. For mRNA quantification, perform single-ended sequencing to generate Fastq files. Ensure a minimum of 50 million reads for each sample.

NOTE: Refer to **Figure 3** for a schematic illustrating the workflow used to process RNA-Seq data and to quantify the expression of differentially expressed transcripts. Sequence data, in the form of Fastq files, are subjected to quality control procedures; >80% of the reads should yield a Phred score of 30 to be considered appropriate for subsequent analysis. The sequences are also preprocessed (trimmed) using Trimmomatic[18] to remove adaptor sequences and filter out low-quality reads.

4.3. Perform RNA-Seq alignment and analysis on the fastq generated files using any capable software program (e.g., DNAStar[19,20] or Partek[21]). Follow the program-specific steps using the default settings to align the fastq files to the mouse reference genome (GRCm38/mm10).

NOTE: Using DNAStar as an example, the general workflow is described below (**Supplemental Figure 1**).

4.3.1. Select the analysis method, **RNA-Seq**.

4.3.2. Select the reference genome, **Mouse**.

4.3.3. Upload the BED file if provided one by the sequencing core.

4.3.4. Upload the fastq sequencing files, assigning them unique replicate names.

4.3.5. Group-replicate the fastq files and designate them to a replicate set (i.e., **GFP**, **CRE**)

NOTE: Each alignment program has its specific steps, and the user must consult with the program user guide for the program-specific protocol. The program will then generate gene-specific raw count data from these Fastq files.

4.4. Perform statistical and normalization analysis (DESeq2, EdgeR) on the raw count data using any capable software programs, as described in 4.3, with the Ad5CMV-eGFP sample set as the control data set and Ad5CMV-Cre set as the test data set to identify differential gene expression signals with robust statistical power[22,23].

4.4.1. Select **GFP fastq files** as the control data set.

4.4.2. Select **DESeq2** as the statistical and normalization method**.**

4.4.3. Start assembly and analysis.

NOTE: Each alignment program has its specific steps, and the user must consult with the program user guide for the program-specific protocol. The program will then generate gene-specific raw count data from these Fastq files. The statistical and normalization analysis is a built-in step in many programs, as shown in the example here, within the sequence alignment protocol. If an

alternative sequence alignment software program is used that does not offer this subsequent built-in step, perform the statistical and normalization analysis on the raw count data at the terminal level using the DESeq2 or EdgeR coding packages written in R, freely available for download on Bioconductor.org.

4.5. Use these approaches to identify changes representing at least a 1.5 fold increase or decrease relative to the control (in this case, cells transduced with the Ad5CMV-eGFP virus). Use only those differentially expressed genes (DEGs) determined to be statistically significant that show ≥1.5-fold changes and a *p*-value ≤ 0.05 or a padj of ≤ 0.1 for subsequent functional enrichment analysis.

NOTE: This will generate a list of DEG genes and their statistical power for functional enrichment analysis.

4.6. Perform functional enrichment analysis on statistically significant *Erbb4*-mediated DEG identified in 4.4 with a ranked gene list file using any of the freely available web-based tools. Determine biological and pathway significance of *Erbb4* gene loss through gene ontology datasets integrated in these open-access functional enrichment analysis tools[24-27] (see the **Table of Materials** for examples and **Figure 3** for an example workflow using Panther).

4.6.1. Export the data obtained in step 4.4 as a spreadsheet.

4.6.2. Rank the data by log2 fold change, p/padj value, or both.

4.6.3. Be sure to remove all non-statistically significant data.

4.6.4. Export the ranked gene list with gene ID only as a .txt file and upload it to the website.

NOTE: Use only statistically significant DEG (p/padj values < 0.05 or 0.1, respectively) to generate a ranked input gene list using log2 fold changes (highest to lowest), p/padj-values (lowest to highest) or both [(-log10(pval)*sign(log2FC)]. There are several choices to generating a ranked gene list, and the ideal choice should be empirically determined for the dataset and the question being asked. The specific type of functional enrichment analysis tool being used can also assist in determining the appropriate type of rank gene list. For additional resources on RNA-Seq, see the following papers[28-30].

5. Orthotopic allografting of MPNST cells with ablated *Erbb4* alleles and analysis of the effects of *Erbb4* ablation

5.1. Before performing orthotopic allografting of sorted MPNST cells, ensure that all procedures are reviewed and approved by the Institutional Animal Care and Use Committee, and that all procedures are performed by properly trained personnel.

5.2. On the day of injection, remove low passage cells (approximately 85% confluency) from

cell culture plates or flasks using a non-enzymatic cell dissociation solution (e.g., a mixture of chelators; see the **Table of Materials**) and count the cells using a hemocytometer. For orthotopic injections into the sciatic nerve, reconstitute the cells at 16,667 cells/mL (50,000 cells per 3 µL for each animal) in DMEM-10[31]. Keep the cells on ice.

NOTE: Some cultures will not successfully establish grafts unless the cells are injected in low-growth factor basement membrane matrix. The requirement for a basement membrane matrix (10–50%) must be empirically determined.

5.3. Assess *in vivo* allograft growth potential in post-infected cells by injecting MPNST cells into the sciatic nerve of 8–10 anesthetized Hsd: Athymic Nude-Foxn1^{nu} mice per cohort (aged 4–8 weeks) as described previously[31].

NOTE: To determine the number of experimental animals needed for statistical significance, it is recommended to use G*Power3, a freely available software[32].

5.4. Monitor the animals closely twice daily for the first week post-injection for any signs of pain. Thereafter, monitor the grafted mice three times per week for caliper measurements and assess body condition scores (BCSs) as previously described[5,31]. As outlined in IACUC guidelines, euthanize animals with a BCS of 2 or less.

5.5. As grafted cells grow at different rates, determine graft times empirically using control (unmodified) cells before performing experiments described in this section. To collect the grafts at the experimental endpoint, euthanize the mice humanely using carbon dioxide inhalation followed by cervical dislocation as a secondary measure. Record the final volume and mass measurements of each graft.

NOTE: As unmodified P_0-GGFβ3;*Trp53*$^{+/-}$;*Erbb4*$^{fl/fl}$ MPNST cells typically reach the maximum size allowed by IACUC within 30–45 days, a typical timeline is around 30–45 days after injection.

5.6. Isolate and section tissue as described in steps 1.6-1.8. Fix part of the graft tissue overnight in 4% paraformaldehyde (**Figure 2**) and then embed it in paraffin. Prepare 5 µm sections from the FFPE tissue and mount them on slides. Perform H&E staining and other necessary immunostaining to confirm that the graft tissue is composed of tumor cells as described in 1.8.1. Snap-freeze the rest of the tumor tissue for downstream analyses, such as validating the loss of *Erbb4* expression and assessing the effects of *Erbb4* loss on the expression of other *Erbb* family members.

NOTE: Confirmation of tumor cells in the graft tissue must be done because immunodeficient mice are prone to develop neoplasms. In the case of small grafts, it is important to ensure that scar tissue or inflammation is not mistaken for a neoplasm.

5.6.1. Perform standard IHC staining on the FFPE tissue to compare the expression of proteins of interest in allografts grown from Ad5CMV-eGFP and Ad5CMV-Cre/eGFP treated cells. Stain the

excised graft tissue using erbB4-specific antibodies to confirm differences in *in vivo* erbB4 expression between the two experimental conditions. Determine the proliferative index via Ki67 staining and the level of apoptosis via terminal deoxynucleotidyl transferase-mediated dUTP nick-end labeling (TUNEL) staining.

NOTE: Any protein target of interest can also be assessed via IHC. For example, assess vascular density by immunostaining allografts with an anti-CD31 antibody (1:50 dilution) to determine in vivo vascular microenvironment differences mediated by gene ablation. The number of vascular profiles per 10x field can be counted for quantification. For these IHC-based assays, follow standard IHC protocols for the staining procedures and the manufacturer's protocol for TUNEL staining. For quantification of images, use the ImageJ plug-in "automated counting of single-color image."

REPRESENTATIVE RESULTS:

Figure 4 illustrates a typical result obtained when transducing P_0-GGFβ3;*Trp53*$^{-/+}$;*Erbb4*$^{fl/fl}$ MPNST cells with either the Ad5CMV-eGFP adenovirus or Ad5CMV-Cre/eGFP adenovirus (**Figure 4A**). Cultures are viewed with fluorescence microscopy to identify eGFP-expressing cells and by phase-contrast microscopy to determine the total number of cells present in the same field at 10x (top) and 40x (bottom). The percentage of cells expressing eGFP can then be calculated if desired. Representative FACS output data are shown in **Supplemental Figure S2**. Following FACS, the percentage of eGFP-expressing cells will be markedly increased, with virtually all the cells in each field expressing eGFP. Typical PCR genotyping results expected after Cre-mediated gene ablation, depending on the transfection efficiency, are complete gene knockout (100% efficiency) or a heterogeneous population of induced and uninduced cells (<100% efficiency) compared to control transduction results (GFP only, fl/fl) (**Figure 4B**). **Figure 4C** illustrates the characteristic histopathology found in orthotopic allografts of P_0-GGFβ3;*Trp53*$^{+/-}$;*Erbb4*$^{fl/fl}$ MPNSTs compared to the tumors derived from the original GEM animal models.

In these experiments, *Erbb4* ablation resulted in decreases in cellular proliferation and cellular density *in vitro* and *in vivo*, increases in TUNEL labeling indices *in vivo*, and decreased vascular density *in vivo*. **Figure 5** illustrates representative results obtained with an image-based automated cytometer showing decreased cellular proliferation in Ad5CMV-Cre ablated cells vs. control Ad5CMV-GFP transduced cells (**Figure 5A**); these experiments were performed with early passage cultured cells. Expression of ErbB4 via immunohistochemistry in P_0-GGFβ3;*Trp53*$^{+/-}$;*Erbb4*$^{fl/fl}$ MPNST cells transduced with Ad5CMV-Cre or eGFP virus was decreased in the resultant Ad5CMV-Cre transduced allografts compared to control Ad5CMV-eGFP treated allograft tumors (**Figure 5B**). Vascular density was assessed via immunoreactivity detection for CD31; vascular density can be seen to be markedly reduced in allografts of Ad5CMV-Cre transduced cells (**Figure 5C**). Signal intensity can be quantified, if desired, using ImageJ.

FIGURE LEGENDS:

Figure 1: Punnet square calculations of the ratios of expected genotypes when generating and crossing P_0-GGFβ3;*Trp53*$^{+/-}$ mice with *Erbb4*$^{fl/fl}$ mice (F1). Punnet square calculations of the ratios of expected genotypes when generating and maintaining P_0-GGFβ3;*Trp53*$^{-/+}$;*Erbb4*$^{fl/+}$ with each

other (F2). Abbreviation: fl = Floxed.

Figure 2: Workflow of the process used to ablate floxed *Erbb4* alleles in early passage cultures of MPNST cells derived from P_0-GGFβ3;*Trp53*$^{-/+}$;*Erbb4*$^{fl/fl}$ mice. (**A**) Harvest the tumor expressing the floxed gene. (**B**) Create early passage cultures from the excised tumor. (**C**) Infect early passage cultures to ablate the floxed gene and perform downstream assays. Abbreviations: MPNST = malignant peripheral nerve sheath tumor; IHC = Immunohistochemistry; PFA = Paraformaldehyde; FFPE = Formalin-fixed paraffin-embedded; H&E = Hematoxylin and eosin; FACS = fluorescence-activated cell sorting; GFP = green fluorescent protein; K/O = knockout; PCR = polymerase chain reaction.

Figure 3: Schematic illustrating the RNA-Seq workflow. The workflow is used to identify differentially expressed transcripts between control (GFP-induced) and *Erbb4*-null (Cre-induced) cells and the resultant biological significance. Abbreviations: GFP = green fluorescent protein; RNA-Seq = RNA sequencing.

Figure 4: Representative transduction efficiency results assessed by microscopy in P_0-GGFβ3;*Trp53*$^{-/+}$;*Erbb4*$^{fl/fl}$ MPNST cells. (**A**) Cells transduced with either Ad5CMV-eGFP adenovirus or Ad5CMV-Cre/eGFP adenovirus. (**B**) PCR results of potential gene populations post-Ad5CMV infection. (**C**) Characteristic histopathology comparing the tumors generated in the originating GEM models to the orthotopically allografted P_0-GGFβ3;*Trp53*$^{-/+}$;*Erbb4*$^{fl/fl}$ MPNST cells via H&E staining. Images were taken at 40x. Isotype-matched negative control antibodies were used for control staining. Scale bars = 400 μm (**A**, upper panel); 100 μm (**A**, lower panel), 20 μm (**C**). Abbreviations: MPNST = malignant peripheral nerve sheath tumor; GFP = green fluorescent protein; BF = brightfield; FACS = fluorescence-activated cell sorting; Neg Ctrl = negative control; PCR = polymerase chain reaction; GEM = genetically engineered mouse; fl = floxed.

Figure 5: Representative results obtained in cultured MPNST early passage cultures and orthotopically allografted MPNST cells following transduction with either Ad5CMV-eGFP or Ad5CMV-Cre/eGFP. (**A**) Proliferation assay of cultured MPNST cells demonstrating decreased cellular density in cells transduced with Ad5CMV-Cre/eGFP compared to those transduced with Ad5CMV-eGFP. Quantified data are graphed on days 1, 3, and 5 (left). Day 1 and Day 5 confluency images taken on the image-based automatic cytometer are shown on the right (Images taken at 4x magnification with brightfield microscopy). Error bars represent the standard error of the mean (SEM) of at least 3 different independent experiments. (**B**) Representative ErbB4 staining in allograft tumors transduced with Ad5CMV-eGFP or Ad5CMV-Cre/eGFP adenovirus taken at 20x magnification. Red channel (Alexa 564, CD31), blue channel (Hoechst, nuclei). (**C**) Representative images of vascular density in allografts of P_0-GGFβ3;*Trp53*$^{+/-}$;*Erbb4*$^{fl/fl}$ MPNST cells transduced with Ad5CMV-eGFP versus Ad5CMV-Cre/eGFP virus. Images were taken at 40x. Isotype-matched negative control antibodies were used for control staining. Scale bars = 100 μm. Abbreviations: MPNST = malignant peripheral nerve sheath tumor; eGFP = enhanced green fluorescent protein; IgG = immunoglobulin G; NEG = negative control; CD = cluster of differentiation.

Supplemental Figure S1: Schematic illustrating a sequence alignment and analysis workflow. The workflow used in DNAStar to align and analyze RNA-sequencing files (fastq files). Abbreviations: GFP = green fluorescent protein; RNA-Seq = RNA sequencing., DEG = differentially expressed genes.

Supplemental Figure S2: Representative FACS data from early passage cultures using green fluorescent protein. (**A**) GFP-expressing cells are sorted by FACS after setting fluorescent gate parameters from non-infected cells. (**B**) After the appropriate detection gate is set, GFP-positive (transduced) cells are separated from GFP-negative (non-transduced) cells. Abbreviations: SSC-A = side scatter–area of peak; FSC-H = forward scatter–height of peak; FSC-W = forward scatter–width of peak; GFP = green fluorescent protein; FACS = Fluorescence-activated cell sorting.

DISCUSSION:

The detailed methods presented here were developed using a GEM model of MPNSTs. However, if the tumor tissue of interest can be dispersed into individual cells, these methodologies are easily adaptable for various tumor types arising in GEMs. It is important to ensure that the floxed allele does not result in i) decreased survival that can make it difficult to obtain sufficient mice to screen for tumors, or ii) increased tumor latency that can make it difficult to obtain enough tumor-bearing mice. If the floxed allele does not affect survival, the survival of both cohorts will be equivalent. If it has no effect on tumor latency, equivalent numbers of tumor-bearing mice should arise in both cohorts with a similar time course.

Similar approaches have been used to study neurofibromas and MPNSTs using conditional knockouts and tamoxifen-inducible Cre animals to generate inducible conditional knockout animals[33,34]. The difference between these studies and this one, aside from the use of tamoxifen for Cre induction as previously discussed, is that these studies focus on tumor development with a tissue-specific knockout of NF1. As this study and these other studies also use GEMM-generated tumors, the difference lies with the question being asked. In this protocol, we are not studying the role that NF1 loss plays in MPNST pathogenesis but are instead studying the role that a specific gene (*Erbb4*) in GEMM-generated MPNSTs exerts on *in vivo* tumor growth, which would otherwise be impossible due to being embryonic lethal. Furthermore, this protocol avoids the use of tamoxifen for those approaches requiring such parameters.

Others have studied established human MPNST cell lines in xenograft models[35]. That study differs from this one in that the grafted cells used are well-studied but high-passage human MPNST cell lines, and it focuses on establishing drug responses in xenografts. Those researchers are not studying the role of a specific gene in these MPNST cells for *in vivo* growth and the effects of gene loss on drug response. Another study similar to this one was performed by Dodd et al., using adenovirus Cre recombinase (Ad-Cre)-mediated NF1 loss in a temporal and spatial dependent manner, again a powerful method for expanding MPNST translational efforts[36]. The study focused on the role of *NF1* and *Ink4a/Arf* loss, two very commonly co-deleted genes in human MPNSTs, in the sciatic nerve by Ad-Cre injection. The P_0-GGFβ3;*Trp53*$^{+/-}$;*Erbb4*$^{fl/fl}$ mice described in this study could be used in this fashion by injecting Ad-Cre into Schwann cell precursor lineages. However, the questions asked in this study are not focused on the evolutionary role of *Erbb4* on

MPNST initiation but on how MPNSTs may hijack *Erbb4* signaling for tumor growth advantage.

There are alternatives to the approach described here, including knocking down gene expression via RNA interference (RNAi) or inactivating the gene of interest with CRISPR in human cancer cell lines. These alternative approaches are valuable and can be partnered with gene ablation in cells derived from GEM tumors to verify that the effects observed in mouse tumor cells are recapitulated in their human counterparts. However, there are some clear advantages to the methodology described here. First, genetically ablating floxed genes in GEM cancer cells is rapid and produces complete inactivation of the targeted gene. In contrast, it is often observed that the use of short hairpin RNAs results in only a partial knockdown of gene expression. Although CRISPR can produce complete gene inactivation, the identification of clones that have complete inactivation requires a prolonged selection process.

Further, multiple clones must be examined to ensure that the effects resulting from CRISPR ablation do not differ between different clones. Second, the ability to ablate floxed alleles in early passage GEM tumor cultures is advantageous as this minimizes the possibility of selecting for distinct tumor cell subpopulations that grow effectively in culture. In comparison, human cell lines, which have typically been maintained in culture for years, are often derived from distinct subpopulations that are well adapted for culture and frequently undergo genetic drift during this process. This results in these cell lines developing new mutations that were not present in their parent tumor. Finally, although the grafting of GEM tumor cells into immunodeficient mice is described in this manuscript, it is noted that GEM tumor cells derived from tumors arising in inbred mouse strains can be allografted into mice of the same strain. This would allow the investigator to assess tumor biology in animals with an intact immune system in the presence or absence of the targeted gene.

The critical step in the protocol described here is the ablation of the floxed gene with Ad5CMV-Cre/eGFP and ensuring the survival of the tumor cells following gene ablation and FACS. As this is a process that is dependent on the ability of Cre recombinase to ablate the floxed gene, it is potentially subject to some of the same problems that can be encountered when ablating a floxed gene *in vivo*; these issues would manifest as an incomplete ablation of the targeted allele. Note that the ability to purify cells that have been successfully transduced with the eGFP-expressing adenoviral vector does appear to minimize mosaicism compared to *in vivo* gene ablation with $CreER^{T2}$. However, in the case of targeted genes encoding proteins, such as ErbB4 that are expressed on the cell surface, it may be possible to further ensure the loss of the targeted gene by performing FACS utilizing both eGFP and an antibody recognizing the protein of interest (i.e., sort the eGFP-positive/erbB4-negative cells).

Because, as was noted in the introduction, many of the proteins targeted therapeutically by monoclonal antibodies are cell surface proteins, this approach should frequently be feasible. It should also be noted that it is important to let the tumor cells recover for at least 2–3 days after FACS if RNA-Seq is to be performed on them to assess the effect that gene ablation has had on the transcriptome. RNA-Seq datasets obtained very soon after FACS often show more variability in gene expression between biological replicates in some cell types. This may be a consequence

of the trauma that cells suffer when going through FACS; hence, the cells must be allowed a recovery period after this process. RNA-Seq datasets can be analyzed using DESeq2, which uses the negative binomial distribution and a shrinkage estimator for the distribution's variance. In these analyses, samples are sorted according to their *q-value*, which is the smallest false discovery rate (FDR) at which changes in transcript levels are significant; FDRs are calculated using the Benjamini-Hochberg multiple testing adjustment procedure. Alternatively, DEGs can be identified using other available software capable of RNA-Seq analysis workflows.

For this MPNST animal model, identifying the experimental endpoint requires an understanding of the natural history of the neoplasms in the animal model that is being used. The natural history of MPNSTs in this GEM was determined by following the survival of a series of 44 P_0-GGFβ3 mice[6] and 19 P_0-GGFβ3;*Trp53*$^{+/-}$ mice[7] and then performing complete necropsies on all of these animals when they reached their survival endpoint. The typical survival times and the location where MPNSTs typically arose were determined in each animal model. In most of these mice, MPNSTs arose in the trigeminal nerve. MPNSTs arising in the trigeminal nerve typically produced ptosis associated with corneal cloudiness (a result of problems with tear distribution produced by the ptosis), which provided a clinically useful sign to identify tumor-bearing mice. Tumor diagnosis should be confirmed by performing H&E stains and several additional diagnostic stains (S100, nestin Sox 10, H&E, Mart1) followed by an examination by a qualified veterinary or human pathologist. This is also important because the *Trp53* null allele in this model predisposes the mice to the development of other neoplasms such as lymphomas, and these tumors must be distinguished from MPNSTs.

Finally, this methodology has several potential applications not yet explored but may be feasible in future investigations. For example, neuregulin 1 (NRG1), the ligand that activates both erbB3 and erbB4, promotes the migration of MPNST cells in a chemotactic fashion; both erbB3 and erbB4 are located in the invadopodia of MPNST cells[37]. However, it is not clear whether erbB3 or erbB4 mediates the chemotactic response to NRG1. Consequently, cells in which erbB4 is ablated with this methodology can be used to address this question. A natural follow-up to these experiments is to assess whether erbB4 is required for metastasis using the commonly utilized approach in which tumor cells are injected via the tail vein and the number of pulmonary metastases then assessed. This methodology offers a clear advantage over other approaches, such as using shRNAs to knock down *erbB4* expression because shRNA expression is often silenced in cells after a while. Further, early passage cultures are anticipated to contain a mixture of tumor-derived subpopulations, including subpopulations of cells prone to metastasis. Performing metastasis assays with cells prepared using the methodology described here will allow an assessment of metastatic potential that is more representative of the parent tumor than an established cell line. This is, of course, just one example of the future applications that could utilize this methodology. We hope that other investigators will combine this methodology with problems of particular interest to enhance the ability to identify proteins that are key therapeutic targets in human cancers.

ACKNOWLEDGMENTS:

This work was supported by grants from the National Institute of Neurological Diseases and

Stroke (R01 NS048353, R01 NS109655), the National Cancer Institute (R01 CA122804), the Department of Defense (X81XWH-09-1-0086, W81XWH-11-1-0498, W81XWH-12-1-0164, W81XWH-14-1-0073, and W81XWH-15-1-0193), and The Children's Tumor Foundation (2014-04-001 and 2015-05-007).

DISCLOSURES:

The authors have no conflicts of interest to disclose.

REFERENCES:

1 Ricciuti, B. et al. Antibody-drug conjugates for lung cancer in the era of personalized oncology. *Seminars in Cancer Biology.* **69**, 268–278 (2019).

2 Litak, J., Mazurek, M., Grochowski, C., Kamieniak, P., Rolinski, J. PD-L1/PD-1 axis in glioblastoma multiforme. *International Journal of Molecular Sciences.* **20** (21), 5347 (2019).

3 Roskoski, R., Jr. Properties of FDA-approved small molecule protein kinase inhibitors. *Pharmacological Research.* **144**, 19–50 (2019).

4 Heffner, C. S. et al. Supporting conditional mouse mutagenesis with a comprehensive cre characterization resource. *Nature Communications.* **3**, 1218 (2012).

5 Longo, J. F. et al. ErbB4 promotes malignant peripheral nerve sheath tumor pathogenesis via Ras-independent mechanisms. *Cell Communication and Signaling.* **17** (1), 74 (2019).

6 Kazmi, S. J. et al. Transgenic mice overexpressing neuregulin-1 model neurofibroma-malignant peripheral nerve sheath tumor progression and implicate specific chromosomal copy number variations in tumorigenesis. *American Journal of Pathology.* **182** (3), 646–667 (2013).

7 Brosius, S. N. et al. Neuregulin-1 overexpression and Trp53 haploinsufficiency cooperatively promote de novo malignant peripheral nerve sheath tumor pathogenesis. *Acta Neuropatholica.* **127** (4), 573–591 (2014).

8 Ducatman, B. S., Scheithauer, B. W., Piepgras, D. G., Reiman, H. M., Ilstrup, D. M. Malignant peripheral nerve sheath tumors. A clinicopathologic study of 120 cases. *Cancer.* **57** (10), 2006–2021 (1986).

9 Gassmann, M. et al. Aberrant neural and cardiac development in mice lacking the ErbB4 neuregulin receptor. *Nature.* **378** (6555), 390–394 (1995).

10 Tidcombe, H. et al. Neural and mammary gland defects in ErbB4 knockout mice genetically rescued from embryonic lethality. *Proceedings of the Nationall Academy of Sciences of the United States of America.* **100** (14), 8281–8286 (2003).

11 Golub, M. S., Germann, S. L., Lloyd, K. C. Behavioral characteristics of a nervous system-specific erbB4 knock-out mouse. *Behavioral Brain Research.* **153** (1), 159–170 (2004).

12 Huijbregts, R. P., Roth, K. A., Schmidt, R. E., Carroll, S. L. Hypertrophic neuropathies and malignant peripheral nerve sheath tumors in transgenic mice overexpressing glial growth factor beta3 in myelinating Schwann cells. *Journal of Neuroscience.* **23** (19), 7269–7280 (2003).

13 Jackson-Fisher, A. J. et al. Formation of Neu/ErbB2-induced mammary tumors is unaffected by loss of ErbB4. *Oncogene.* **25** (41), 5664–5672 (2006).

14 Byer, S. J. et al. Tamoxifen inhibits malignant peripheral nerve sheath tumor growth in an estrogen receptor-independent manner. *Neuro-oncology.* **13** (1), 28–41 (2011).

15 Kang, Y., Pekmezci, M., Folpe, A. L., Ersen, A., Horvai, A. E. Diagnostic utility of SOX10 to

distinguish malignant peripheral nerve sheath tumor from synovial sarcoma, including intraneural synovial sarcoma. *Modern Pathology.* **27** (1), 55–61 (2014).

16 Longo, J. F. et al. Establishment and genomic characterization of a sporadic malignant peripheral nerve sheath tumor cell line. *Scientific Reports.* **11** (1), 5690 (2021

17 Chomczynski, P. A reagent for the single-step simultaneous isolation of RNA, DNA and proteins from cell and tissue samples. *Biotechniques.* **15** (3), 532–534, 536–537 (1993).

18 Bolger, A. M., Lohse, M., Usadel, B. Trimmomatic: a flexible trimmer for Illumina sequence data. *Bioinformatics.* **30** (15), 2114–2120 (2014).

19 Grozdanov, P. N., Li, J., Yu, P., Yan, W., MacDonald, C. C. Cstf2t regulates expression of histones and histone-like proteins in male germ cells. *Andrology.* **6** (4), 605–615 (2018).

20 Kaur, S. et al. CD63, MHC class 1, and CD47 identify subsets of extracellular vesicles containing distinct populations of noncoding RNAs. *Scientific Reports.* **8** (1), 2577 (2018).

21 Avraham, O. et al. Satellite glial cells promote regenerative growth in sensory neurons. *Nature Communications.* **11** (1), 4891 (2020).

22 Love, M. I., Huber, W., Anders, S. Moderated estimation of fold change and dispersion for RNA-seq data with DESeq2. *Genome Biology.* **15** (12), 550 (2014).

23 Lin, Y. et al. Comparison of normalization and differential expression analyses using RNA-Seq data from 726 individual *Drosophila melanogaster*. *BMC Genomics.* **17**, 28 (2016).

24 Eden, E., Navon, R., Steinfeld, I., Lipson, D., Yakhini, Z. GOrilla: a tool for discovery and visualization of enriched GO terms in ranked gene lists. *BMC Bioinformatics.* **10**, 48 (2009).

25 Huang, D. W. et al. The DAVID Gene Functional Classification Tool: a novel biological module-centric algorithm to functionally analyze large gene lists. *Genome Biology.* **8** (9), R183 (2007).

26 Mi, H., Muruganujan, A., Casagrande, J. T., Thomas, P. D. Large-scale gene function analysis with the PANTHER classification system. *Nature Protocols.* **8** (8), 1551–1566 (2013).

27 Subramanian, A. et al. Gene set enrichment analysis: a knowledge-based approach for interpreting genome-wide expression profiles. *Proceedings of the Nationall Academy of the Sciences of the United States of America.* **102** (43), 15545–15550 (2005).

28 Merico, D., Isserlin, R., Stueker, O., Emili, A., Bader, G. D. Enrichment map: a network-based method for gene-set enrichment visualization and interpretation. *PLoS One.* **5** (11), e13984 (2010).

29 Yoon, S., Kim, S. Y., Nam, D. Improving gene-set enrichment analysis of RNA-Seq data with small replicates. *PLoS One.* **11** (11), e0165919 (2016).

30 Koch, C. M. et al. A beginner's guide to analysis of RNA sequencing data. *American Journal of Respiratory Cell and Molecular Biology.* **59** (2), 145–157 (2018).

31 Turk, A. N., Byer, S. J., Zinn, K. R., Carroll, S. L. Orthotopic xenografting of human luciferase-tagged malignant peripheral nerve sheath tumor cells for in vivo testing of candidate therapeutic agents. *Journal of Visualized Experiments: JoVE.* (49), 2558 (2011).

32 Faul, F. E., E; Lang, AG; Buchner, A. G*Power 3: a flexible statistical power analysis program for the social, behavioral, and biomedical sciences. *Behavior Research Methods.* **39** (2), 175–101 (2007).

33 Chen, Z. et al. Cells of origin in the embryonic nerve roots for NF1-associated plexiform neurofibroma. *Cancer Cell.* **26** (5), 695–706 (2014).

34 Mo, J. et al. Humanized neurofibroma model from induced pluripotent stem cells

delineates tumor pathogenesis and developmental origins. *Journal of Clinical Investigation.* **131** (1), e139807 (2021).
35 Chau, V. et al. Preclinical therapeutic efficacy of a novel pharmacologic inducer of apoptosis in malignant peripheral nerve sheath tumors. *Cancer Research.* **74** (2), 586–597 (2014).
36 Dodd, R. D. et al. NF1(+/-) Hematopoietic cells accelerate malignant peripheral nerve sheath tumor development without altering chemotherapy response. *Cancer Research.* **77** (16), 4486–4497 (2017).
37 Eckert, J. M., Byer, S. J., Clodfelder-Miller, B. J., Carroll, S. L. Neuregulin-1 beta and neuregulin-1 alpha differentially affect the migration and invasion of malignant peripheral nerve sheath tumor cells. *Glia.* **57** (14), 1501–1520 (2009).

Figure 1

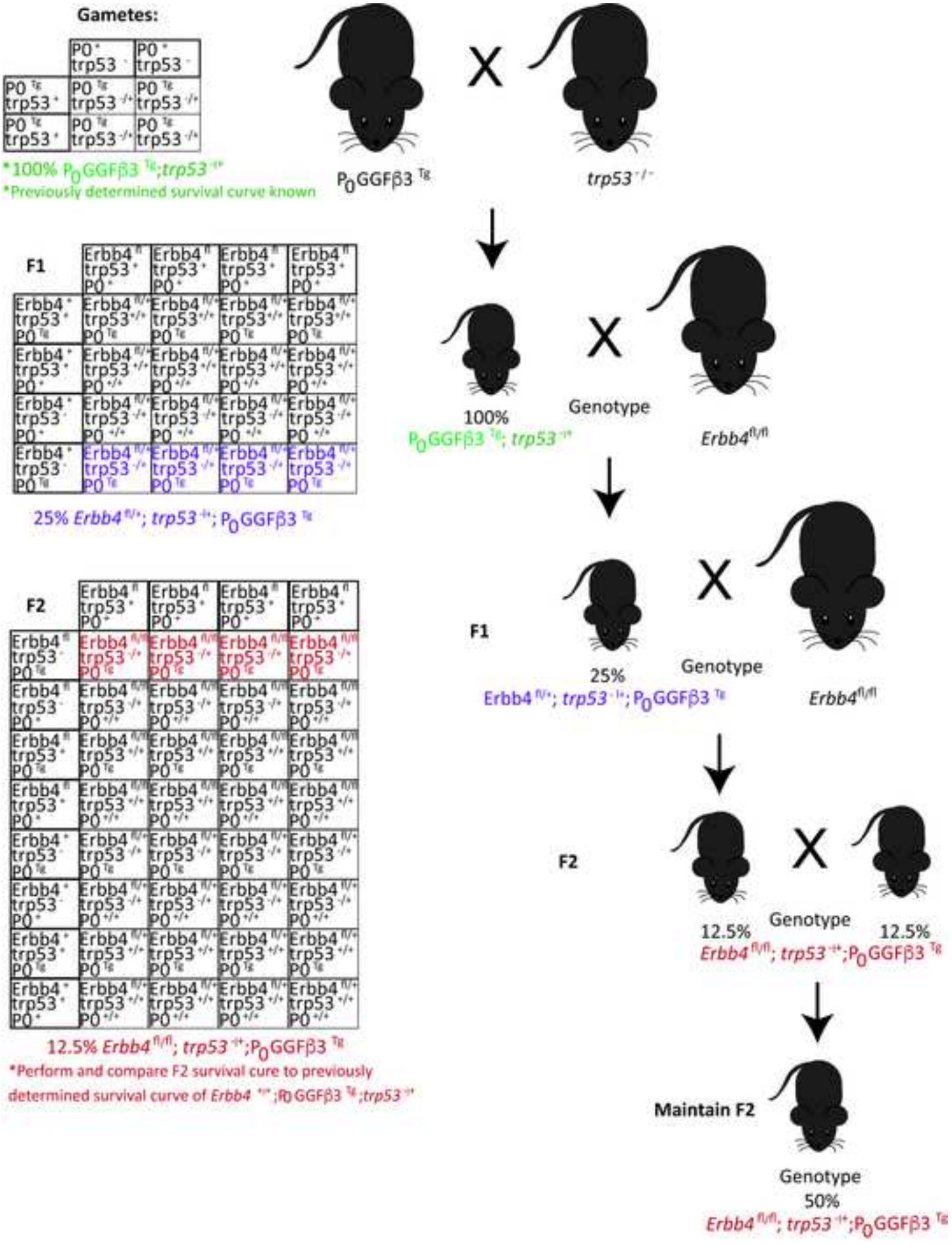

Figure 2

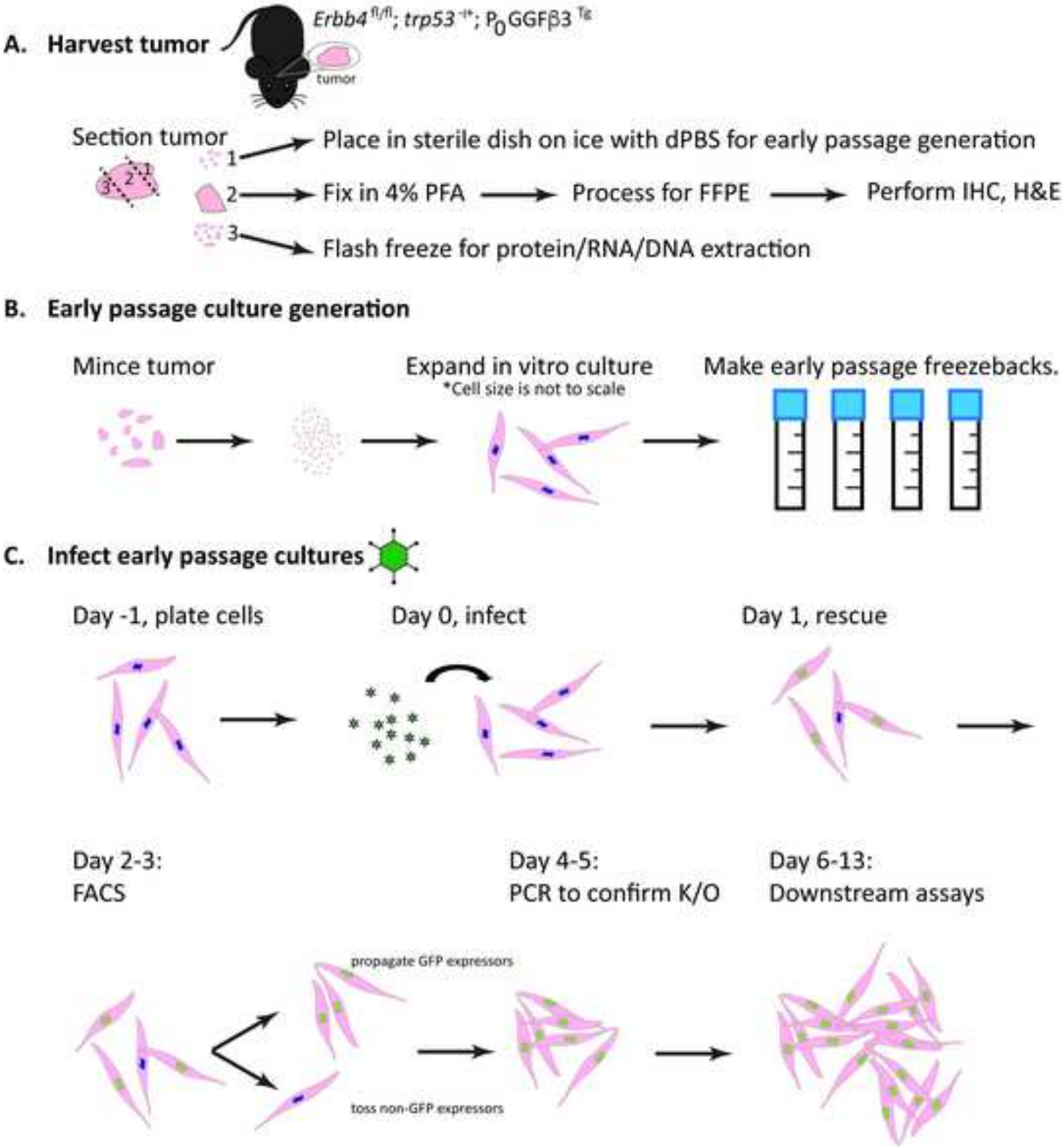

Figure 3

Workflow for RNA Sequencing Analysis

ACQUIRE HIGH QUALITY FASTQ FILES
(Sequencing reads)

↓

ALIGN READS TO REFERENCE MOUSE GENOME
(Specialized assembly software required)

↓

PERFORM DIFFERENTIALY EXPRESSED GENE ANALYSIS
(Specialized software or coding required)
(Alternatively, run count data generated from the previous step in DESeq2 script using R)

↓

GENERATE A RANKED GENE INPUT LIST (.txt)
(Rank high to low using Gene ID, ex: Fold change or p-value)

↓

PERFORM GENE ONTOLOGY
(Web based software required, freely available)

Panther example:

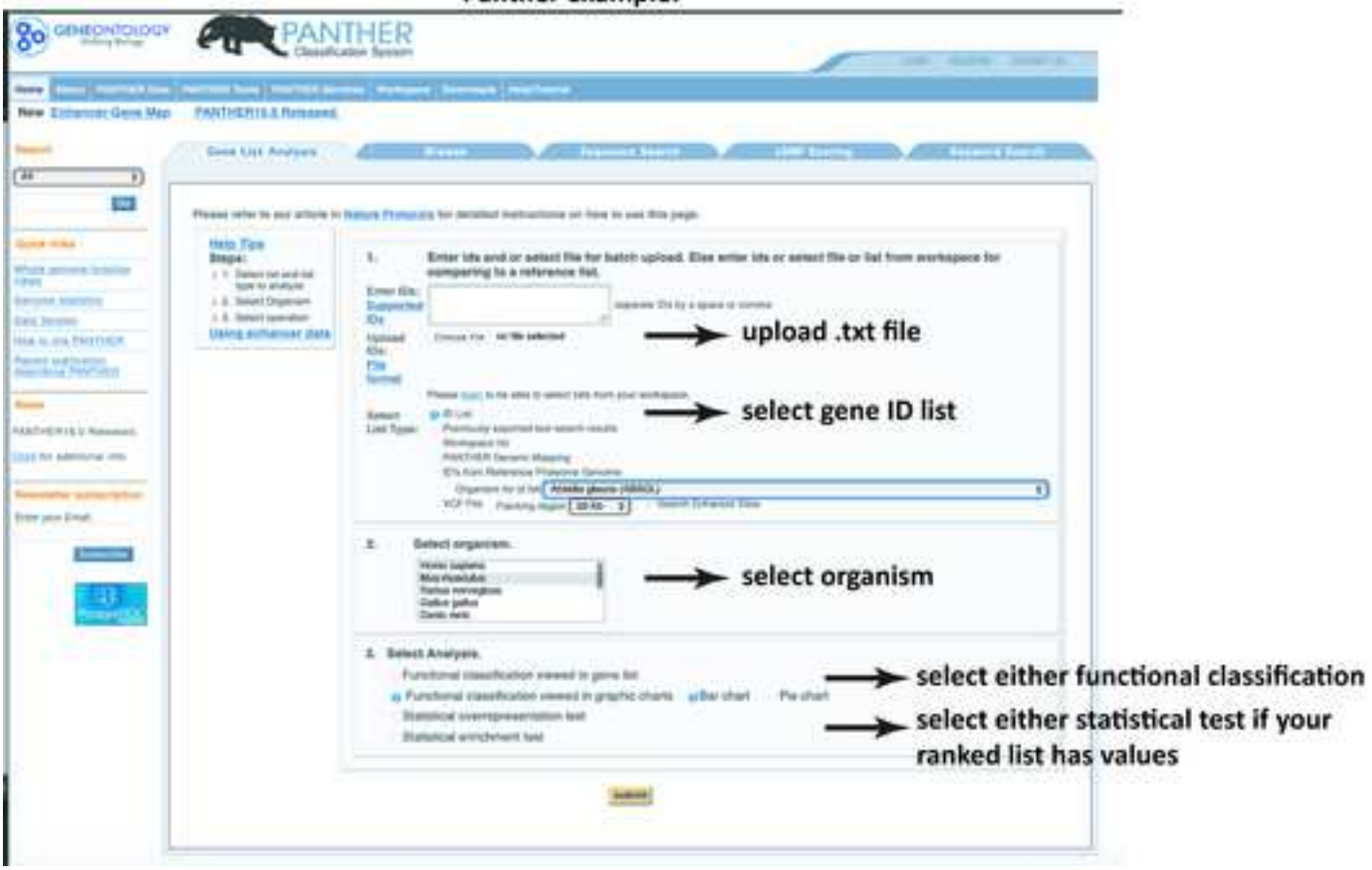

A. Transduction efficiency

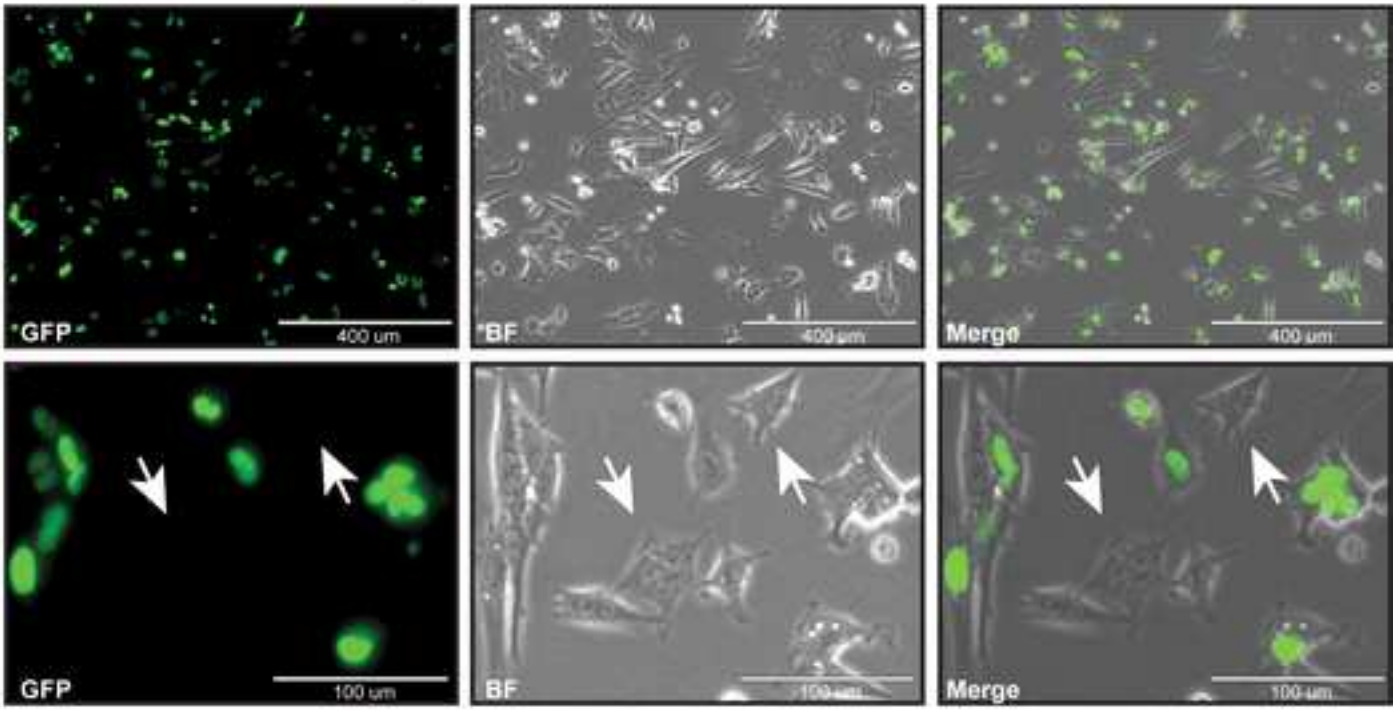

B. PCR Genotyping after Adeno-Cre transduction

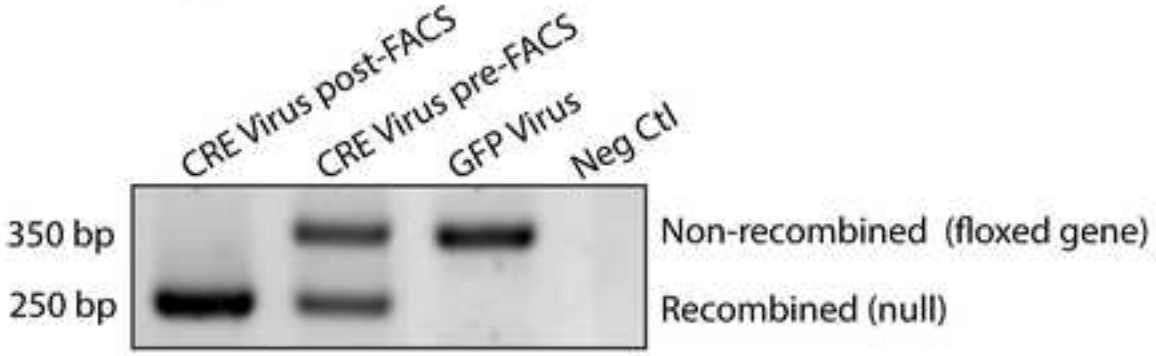

C. Tumor pathology

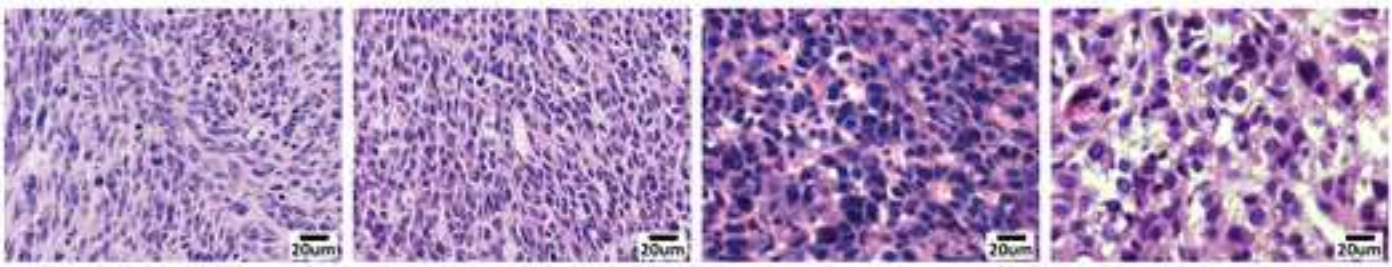

GEM *Erbb4* +/+

GEM *Erbb4* fl/fl

Allograft Ad5CMV GFP

Allograft Ad5CMV CRE

Figure 5

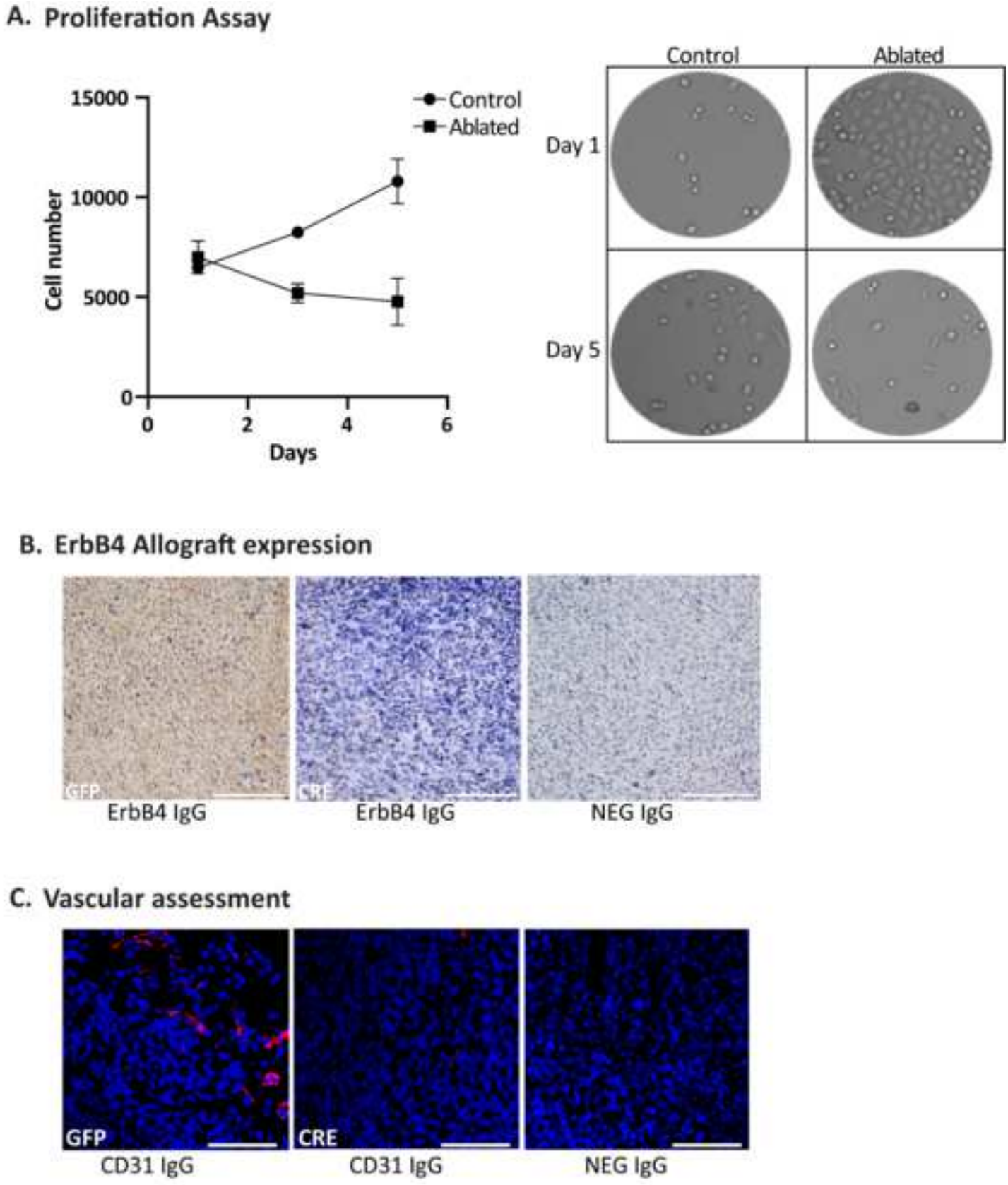

May 31, 2021

Editorial Team.
Journal of Visualized Experiments

Re: Submission JoVE62740

To the Editorial Team:

Thank you for the constructive comments on our manuscript entitled "Defining Gene Functions in Tumorigenesis *In Vivo* and *In Vitro* by *Ex Vivo* Ablation of Floxed Alleles in Malignant Peripheral Nerve Sheath Tumor Cells" and your willingness to consider a revised version of this manuscript. Below we provide a point-by-point response to each of the concerns raised in the original review. We believe that our responses strengthen our manuscript and we are appreciative of the suggestions provided during the initial review process.

Editorial comments:

1. *Please take this opportunity to thoroughly proofread the manuscript to ensure that there are no spelling or grammar issues*.

We have carefully proofread the manuscript and corrected any such errors.

2. *Please rephrase the Summary to clearly describe the protocol and its applications in complete sentences between 10-50 words: "Here, we present a protocol to …"*

We have rephrased the Summary in accordance with these instructions.

3. *JoVE cannot publish manuscripts containing commercial language. This includes trademark symbols (™), registered symbols (®), and company names before an instrument or reagent. Please remove all commercial language from your manuscript and use generic terms instead. All commercial products should be sufficiently referenced in the Table of Materials. For example: Celigo Imager automated cytometer, Nexcelom Bioscience, Trizol, TruSeq, Illumina, HiSeq2500, DNASTAR Lasergene software, DNASTAR, Partek software package, Matrigel, Celigo, etc.*

We have removed all commercial references from the manuscript.

4. *Please revise the text to avoid the use of any personal pronouns (e.g., "we", "you", "our" etc.).*

We have revised the manuscript to remove all personal pronouns.

5. *Please include an ethics statement before your numbered protocol steps, indicating that the protocol follows the animal care guidelines of your institution*.

We now indicate that our protocol was approved by the Medical University of South Carolina IACUC.

6. *Please ensure that all text in the protocol section is written in the imperative tense as if telling someone how to do the technique (e.g., "Do this," "Ensure that," etc.). The actions should be described in the imperative tense in complete sentences wherever possible. Avoid usage of phrases such as "could be," "should be," and "would be" throughout the Protocol. Any text that*

cannot be written in the imperative tense may be added as a "Note." However, notes should be concise and used sparingly. Please include all safety procedures and use of hoods, etc.

We have revised the manuscript so that it is written in the imperative sense.

7. The Protocol should contain only action items that direct the reader to do something. Please move the discussion about the protocol to the Discussion.

We have moved any sections originally in the Protocol that should be in the Discussion to that section.

8. Please add more details to your protocol steps. Please ensure you answer the "how" question, i.e., how is the step performed? Alternatively, add references to published material specifying how to perform the protocol action.

We have added more details to our protocol steps as requested.

9. Line 171-172: Please mention what is monitored in the animals. How is it done?

We have modified the protocol to indicate that we monitor body weight, normal social and grooming behavior and tumor size measurements and clearly indicate what findings in each of these measures is abnormal.

10. Line 186-191: How is the tumor sectioned? Please specify the sizes of sections used for the different analyses mentioned in the steps. Add citations if necessary.

We have revised the protocol to indicate that each tumor is divided into three sections using breadloaf style cuts under sterile conditions as shown in Figure 2A. Section 1 is 10% of total tumor volume, Section 2 is 70% of total tumor volume and Section 3 is 20% of total tumor volume. This is also clarified in Figure 2.

11. Line 192-193: Please mention the specifics of the staining methods (H&E, IHC) used. A citation would suffice. How is the diagnosis confirmed? Are there any specific criteria to confirm the diagnosis?

We have added citations and the following text to the manuscript: "To confirm diagnosis, a qualified veterinary or human pathologist is needed to assess all stained tumor slides following WHO criteria". The details of how we diagnose MPNSTs and grade them is fully described in the quoted reference (Brosius et al *Acta Neuropathologica* 127: 537 (2014)); Brosius et al also includes the references to the WHO diagnostic criteria that we use, which were originally proposed by Scheithauer and Woodruff.

12. Line 205-207: Please mention the volume of PBS used?

We now specify that 10 mL of PBS is used.

13. Line 209: For SI units, please use standard abbreviations when the unit is preceded by a numeral. Abbreviate liters to L to avoid confusion. Examples: 10 mL, 8 µL, 7 cm2 (lines 224, 225, 227, etc.)

We have changed the text as requested.

14. Line 255-256: Please include a reference for genomic DNA isolation.

We have added the requested reference.

15. Line 257-260: Please include the details of the primers used. Specify the working conditions of PCR.

We now provide these details on lines 309 and 172.

16. Line 262-263: Please elaborate on the cell preparation for in vitro assays. Add references if necessary.

We have clarified and simplified the “prepare cells for” text with the following sentence: “Cells are ready for *in vitro* cell-based assays as described below”. There is no additional “prepare” step outside of what is outlined in the proceeding outlined protocol steps, so we changed that wording to avoid confusion.

17. Please include a one-line space between each protocol step.

We have added a one-line space between each protocol step.

Then highlight up to 3 pages of the Protocol (including headings and spacing) that identifies the essential steps of the protocol for the video, i.e., the steps that should be visualized to tell the most cohesive story of the Protocol. Remember that non-highlighted Protocol steps will remain in the manuscript, and therefore will still be available to the reader.

18. Please do not use the &-sign or the word “and” when listing authors in the references. Authors should be listed as last name author 1, initials author 1, last name author 2, initials author 2, etc. Title case and italicize journal titles and book titles. Do not use any abbreviations. Article titles should start with a capital letter and end with a period and should appear exactly as they were published in the original work, without any abbreviations or truncations.

In the original manuscript, Endnote 8 was used to auto-generate the references using the JoVE style output selection. In our resubmission, the most updated version of Endnote 9 was used but did not seem to fix the formatting issue. Is there a more recent JoVE journal output style that you can recommended for the references to avoid these formatting issues?

19. Figure 3: Please use generic terms instead of commercial terms in the figure.

We have replaced the commercial terms with generic terms in the figure.

20. Figure 4: Please include error bars in all the images of the panel.

Scale bars were added to all panels in 4A and bar size information was added to all 4B panels.

21. Figure 5: Does the Y-axis in Figure 5A represent cell numbers? If so, please revise the Y-axis.

Yes, it does. We have revised the figure to clearly indicate this.

22. Please revise the table of the essential supplies, reagents, and equipment. The table should include the name, company, and catalog number of all relevant materials in separate columns in an xls/xlsx file. Please sort the Materials Table alphabetically by the name of the material.

We have revised the table to include this information.

Reviewers' comments:

Reviewer #1:

This paper is well-written and scientifically sound. The methodology reported in this manuscript will be of high interest to the NF1 community and any other individuals using GEMM approaches. For this to be acceptable for publication, several items need to be addressed in the text.

Major comments:

While this reviewer agrees that mosaicism in Cre-based deletion can occur in vivo (as mentioned in lines 124-128), there are some alternative interpretations of the Erbb4 mosaicism phenotype that must be discussed. Alternative interpretations include: 1) the inability of tamoxifen to completely penetrate into the PNF lesion, 2) it is possible that Erbb4 deletion can only be achieved when permissive secondary mutations occur (ie: perhaps due to p53 loss, there is additional (but spontaneous) loss of certain "permissive" genes that will allow the cell to accept Erbb loss. Since this event would occur stochastically, only some cells in the tumor would show Erbb loss following tamoxifen injection), and 3) it is also possible the immune system has selected against Erbb4-null cells, and thus only cells with an additional "permissive" mutation are capable of escaping the immune-editing process to grow into a tumor. Please discuss these other interpretations in the text.

The following text was added: “The mosaicism observed could be a result of inefficient tamoxifen delivery, resulting in differences in recombination efficiency within the tissue. The possibility of spontaneous compensatory mechanisms could further contribute to mosaicism in tamoxifen mediated recombination by bypassing the requirement for Erbb4 expression. It is feasible that loss of *Trp53* by nature makes tumor cells susceptible to additional spontaneous “permissive” mutations confusing the interpretation of the data”.

Also, to provide context that will assist others using Cre-ER approaches, please give an estimate of the penetrance of recombination of the Erbb4 floxed alleles in the in vivo tumors described in lines 124-128 (ie: were 10% of cells recombined, 50% of cells, etc)? Also, please provide references citing additional reports of Cre and/or Cre-ER approaches resulting in mosaicism (statement in line 100).

In our previous efforts with a CreER^{T2} driver, we observed that approximately 50% of the cells had recombined *Erbb4* alleles *in vivo*.

In cells treated with Ad-Cre-GFP in vitro, how many "false positives" do you get - ie: how many cells are GFP positive but do not have deletion of floxed alleles?

In most of the tumors we tested, the number of GFP+/ cells in which *Erbb4* was not recombined was less than 1%, based on immunoblot and immunohistochemical analysis. Curiously, however, we did encounter occasional tumors in which recombination was less efficient (e.g., see the UBI-1 tumor in Fig. 5A of Longo et al *Cell Communication and Signaling* 17: 74 (2019)

and compare it to the UBI-2 and UBI-3 tumors in the same panel). This is why we recommend in the protocol that investigators confirm that their targeted allele was knocked out in each tumor that they study.

The IF of CD31 shown as the "vascular assessment" is odd - why are there no vessels in 2 of the 3 tumors? What is this data attempting to display?

Our data is showing representative qualitative changes in this example. In panel 5C, we are showing representative images of an *Erbb4* expressing and an *Erbb4* null tumor stained with CD31; the 3rd panel is an isotype-matched negative control stain to show antibody specificity. The *Erbb4* null tumor has lower vascularization, and we see only two pieces of vessels in this particular field. We cannot comment on the orientation of the tissue vs vessel.

Minor comments:
Line 386 uses xenografts, but this refers to allografts.

Thank you for catching this. We have corrected this error.

In figures, increase the font size to make the superscripts (fl, +, -, etc) more legible.

These were increased from 12-point to 14-point font.

Reviewer #2:
Manuscript Summary:
The authors describe a methodology by which to derive short term tumor cultures from genetically modified mice and then subsequently ablate a floxed embryonic lethal gene of interest to overcome technical issues associated with embryonically lethality and mosaicism in conditional knockouts. Purified cells can then but utilized for a number of downstream assays to quantify effects of proliferation, viability, the transcriptome, and even orthoptic allograft growth. Overall, the experimental approach is technically sound and documented in a sufficient level of detail such that others should be able to replicate the methodology without difficulty. The protocol is certainly one that will be useful to other scientists to catalyze both basic mechanistic discovery and therapeutic innovation in this space. There are, however, some points below that do need to be addressed in review, which will ultimately make for a stronger manuscript.

Major Concerns:
1. Lines 179 -180: The overwhelming majority of the experimental mice described here developed MPNST in the trigeminal nerve which is quite interesting as this is NOT a common region where MPNSTs typically arise either in other GEM mouse models or human patients. Do the authors have any explanation or hypothesis for the proclivity of MPNSTs to arise in this distinct anatomic compartment in the context of this model? Was there evidence of pre-existing plexiform neurofibroma in the trigeminal nerves of these mice prior to the onset of MPNST?

We agree with the reviewer that the distribution of MPNSTs in P_0-GGFβ3 and P_0-GGFβ3;*Trp53*$^{+/-}$ mice differs from that seen in humans and have commented on this in two previous publications (Kazmi et al *American Journal of Pathology* 182:646 (2013), Brosius et al *Acta Neuropathologica* 127: 573 (2014)). We have added additional text to the Introduction commenting on this difference. The reason for the different distribution is currently unclear. It may be species related. Another (and not mutually exclusive) possibility is that the tumor progenitor cells are enriched in the trigeminal ganglion of mice. We are currently examining

these and other possibilities. In P_0-GGFβ3 mice, MPNSTs do arise within pre-existing neurofibromas in the trigeminal ganglion. This is not the case with P_0-GGFβ3;*Trp53*$^{+/-}$ mice. We previously demonstrated (Brosius et al *Acta Neuropathologica* 127: 53 (2014)) that NRG1 overexpression can substitute for *Nf1* haploinsufficiency in *Trp53*$^{+/-}$ mice to recapitulate the phenotype of *cis-Nf1*$^{+/-}$;*Trp53*$^{+/-}$ mice; in both P_0-GGFβ3;*Trp53*$^{+/-}$ mice and *cis-Nf1*$^{+/-}$;*Trp53*$^{+/-}$ mice, MPNSTs arise *de novo* rather than from a pre-existing neurofibroma.

2. Lines 196-198 "All of these preparations should be examined by a qualified veterinary or human pathologist to confirm the diagnosis." Completely concur, however the authors should also describe what specific diagnostic criteria were applied in this study to confirm the diagnosis of MPNST both in spontaneously arising tumors in the GEM model and in allograft tumors. Miettinen and colleagues recently published a consensus overview for human patients (PMID 28551330) that can also readily be applied in murine models (PMID 31091306). Mitotic figures (number of mitoses per HPF) and the presence or absence of necrosis should be described as this is critical for delineating atypical neurofibroma from low- and high-grade MPNST.

The editors also raised this point. As noted above in our response to them, we have modified the protocol to include the references and a brief description of the diagnostic and grading criteria that we use (WHO diagnostic criteria as originally proposed by Scheithauer and Woodruff).

The authors also mention that the tumors are S100B, nestin and Sox10 to confirm their neural crest/Schwann cell origin (line 194) - these data should be shown in the figures (Figure 4C) for both the spontaneously arising tumors and the allograft tumors to confirm that these expression paradigms are retained. This is particularly important since these mice harbor germline p53 mutations making them potentially susceptible to developing other soft tissue sarcoma that arise from entirely different cells of origin but could look morphologically similar to MPNST by H&E staining alone.

We have referenced this data in the manuscript as that confirmatory component was highlighted in a previous publication.

3. Lines 212- 214 The authors use forskolin to inhibit the growth of contaminating cell types such as fibroblasts, but they present no validation of the purity of culture at the stage when Ad-Cre is administered to ablate the floxed alleles. If not all contaminating cell types have been removed at this stage, and ablation of the floxed allele results in a gain in function, any remaining fibroblasts/stromal cells could have the potential to become transformed themselves and even acquire the capacity to propagate neoplasia when re-implanted in vivo which could confound results.

In preliminary experiments, cultures were immunostained for S100β to assess their purity. We found that forskolin treatment reduced the number of contaminating non-tumor cells to much less than 1%.

4. While P53 mutation does represent an important subset of MPNST, there are some limitations inherent to the genetic alleles used induce plexiform neurofibroma and MPNST in this model. Firstly, patients with NF1 do not typically develop plexiform neurofibroma driven by neuregulin-1 (NRG-1) overexpression in Schwann cells, but rather due to loss of heterozygosity of the NF1 gene itself in Schwann cell progenitors. Secondly, while a subset of NF1-associated MPNST do harbor TP53 mutation as a second hit, this is a relative minority compared to those that arise due to copy number loss of the INK4/ARF (CDKN2A/B) tumor suppressor locus which

is mutated and 70 to 90% of NF1 associated MPNST (PMID 29118384, PMID20722027, PMID 25240281). The author should acknowledge where this model fits into the overall genetic landscape of MPNST (either NF1 or non-NF1 associated) and limitations with respect to the driver mutations used to induce the phenotype relative to what is known to occur in human patients.

We agree with the reviewer that the pathogenesis of most MPNSTs (essentially all in NF1 patients and a major subset of sporadic and radiation-induced MPNSTs) are driven by *NF1* loss together with the variable occurrence of other mutations (TP53, CDNK2A, PTEN, PRC2 components, etc). We have commented on this extensively in multiple other publications from our laboratory and have included those references in the Introduction. The focus of this paper is methodological rather than comparing the characteristics of several well respected MPNST animal model that have been compared and contrasted in detail previously (e.g., see Brossier and Carroll *Brain Research Bulletin* 88:58 (2012), a review article from our lab that provides an extended discussion of this issue). Consequently, here we have focused on methodologies for studying the function of embryonic lethal genes in a tumor setting.

5. *The authors should also point out that a number of other investigators have also described approaches using Ad-Cre ablate floxed alleles to generate neurofibroma/or MPNST. These approaches include Ad-Cre infection of primary murine embryonic dorsal root ganglion nerve root neurosphere cells (PMID 25446898) , skin derived precursor cells (PMID 24285727), recently human IPS cells (PMID 33108355), and even direct injection of Ad-Cre itself into the nerve tissue (PMID 28646022). Each of these approaches comes with their own inherent advantages and disadvantages relative to the approach described here, but the author should make some commentary on this how this methodology fits into the landscape of other approaches to generate MPNST in genetically modified mice.*
The reviewer brings up important points that are helpful to the discussion. The following text was added:
Similar approaches have been used to study neurofibromas and MPNSTs using conditional knockouts and tamoxifen-inducible Cre animals to generate inducible conditional knockout animals (Chen and Mo). The difference with these studies to ours, aside from the use of tamoxifen for Cre induction as we previously discussed, is that these studies focus is tumor development with tissue specific knockout of NF1. As ours and these other studies are also using GEMM-generated tumors, the difference lies with the question being asked. In this protocol we are not studying the role of NF1-null to generate MPNSTs but are studying the role of a specific gene (*Erbb4*) in GEMM-generated MPNST on *in vivo* tumor growth, that would otherwise be impossible due to being embryonic lethal. Furthermore, this protocol avoids the use of tamoxifen, for those approaches requiring such parameters. We are addressing the role other genes may play in the aggressive nature of MPNSTs. Others have studied established human MPNST cell lines in xenograft models (Chau). This study is similar but different from ours in that the grafted cells used are well studied but high passage human MPNST cell lines and the study is centered on establishing drug response in xenografts to establish preclinical drug studies. They are not studying the role of a specific gene in these MPNST cells for *in vivo* growth and the effects of gene loss on drug response. All of these studies are important and offer translational insight on MPNST therapeutics, but they are all distinct studies as well in regard to the specific question they are asking. Another similar study to ours was performed by Dodd, et al also using adenovirus Cre recombinase (Ad-Cre) mediated NF1 loss in a temporal and spatial dependent manner, again a powerful method for expanding MPNST translational efforts. The study is focused on the role of NF1 and Ink4a/Ark loss, two very commonly co-deleted genes in human MPNSTs, in the sciatic nerve through the use of Ad-Cre injection. Our P_0-GGFβ3;*Trp53*$^{+/-}$;*Erbb4*$^{fl/fl}$ could be used in this fashion by injecting Ad-Cre into Schwann cell

precursor lineages but our questions are not focused on the evolutionary role of *Erbb4* on MPNST initiation but how MPNSTs may hijack *Erbb4* signaling for tumor growth advantage.

Minor Concerns:
1. Lines 99 - 101: The authors state that in their opinion, an underestimated issue is the variability by which Cre drivers to ablate floxed alleles in mice resulting in mosaicism for the null mutation in GEM cancer. The authors should provide supporting references to corroborate this statement.

We originally did not highlight this with references since this is a known drawback of Cre drivers as stated on JAX website (https://www.jax.org/news-and-insights/jax-blog/2011/may/slicing-and-dicing-cre-lox-part-1) but we have added a reference and additional text on the topic.

2. Lines 167 - 170: " If the floxed allele does not have an effect on survival, the survival of both cohorts should be equivalent. If it has no effect on tumor latency equivalent numbers of tumor bearing mice should rise in both cohorts with a similar time course." These sentences appear to be inherently obvious and could likely be omitted from the manuscript but will leave that decision to the editor's discretion.

We moved this to the Discussion but are happy to remove if the editor would like us to.

3. Line 171 "Monitor animals several times a week..." should be changed to "Monitor animals several times per week..."

We have made the requested change.

4. Lines 198- 200: "This recommendation reflects the fact that there are a number of diagnostic mistakes in the literature that occurred when this type of expert examination was not undertaken." The author should provide references to support the statement.

We have removed this statement.

5. Lines 260 -261. The authors state that they have found that PCR assays are more specific than antibody approaches and recommend PCR assays always be performed. Is there a particular reason why the authors feel that PCR would be more specific than showing that the protein itself has been knocked out following Ad-Cre genetic ablation? It would seem that examining protein expression itself would be an equally if not more critical test of actually having achieved a successful genetic knockout in the case of a floxed Cre-mediated recombination event. I would suggest amending this to recommend that both PCR and immunoblot assays be performed as validation.

We have altered the text as follows: “Performing PCR and antibody-based approaches to confirm knockouts is recommended”.

6. Several of the images in the figures are quite pixelated, particularly Figure 1 with the Punnett squares for the breeding schema are very difficult to read due to the degree of pixilation and small font. Would recommend this be addressed prior to publication.

The font was increased in Figure 1 from 10 and 12 to 12 and 14 point. The pixel issue may have been due to file compression. The figures are unpixellated on our end. If they still look pixelated

on your end, we will be happy to submit even higher resolution images.

7. Figure 5A - The authors need to describe the statistical approached used to compare control vs ablated across timepoint and how many replicates (data points) are for each time point in each group. Do the error bars represent SEM or SD?

The error bars are SEM. We have added this text to the legend of Figure 5: “Error bars represent standard error of mean (SEM) of at least 3 different independent experiments”.

We hope that the changes we have made in the manuscript have addressed the concerns noted above concerns adequately.

Sincerely,

Steven L. Carroll, MD, PhD
Professor and Chair
Department of Pathology and Laboratory Medicine
Medical University of South Carolina
171 Ashley Avenue, MSC 908
Charleston, SC 29425-9080
Telephone: (843) 792-3121
FAX: (843) 792-0555
E-mail: carrolst@musc.edu

Supplemental Figure S1

Click here to access/download;Supplemental File (Figures, Permissions, etc.);Supplemental Figure 1.tif

4.3) Choose Workflow:
NGen

4.3.1) Choose method:
RNA-Seq

4.3.2) Choose Reference Genome:
Mouse

4.3.3. Choose Bed File
Only if provided one by sequencing core

4.3.4. Upload fastq Files:
Upload control and test technical or biological replicates using unique replicate names.

4.3.5. Group fastq Files:
Group replicates to assign to a replicate set (i.e. GFR or CRE).

4.4.1. Designate Control:
Set control set to GFP.

4.4.2. Designate Statistical/ Normalization Method:
DESeq2 or EdgeR recommended for identifying DEG

4.4.3. Start Assembly:
Select local or cloud depending on your set up.

Supplemental Figure S2

Click here to access/download;Supplemental File (Figures, Permissions, etc.);Supp Figure 2.tif

A

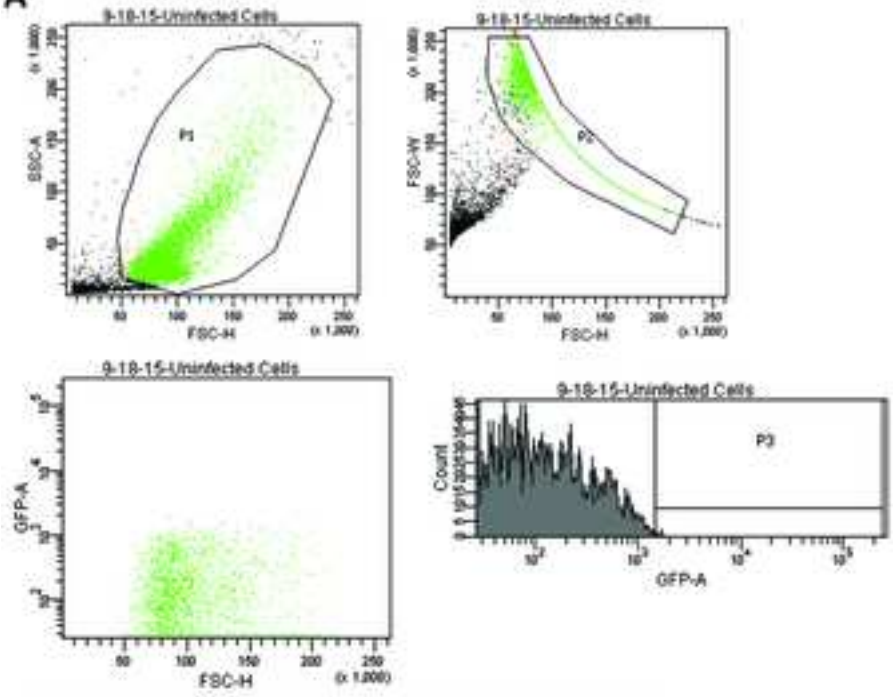

Tube: Uninfected Cells

Population	#Events	%Parent	%Total
All Events	10,000	####	100.0
P1	7,532	75.3	75.3
P2	7,460	99.0	74.6
P3	3	0.0	0.0

B

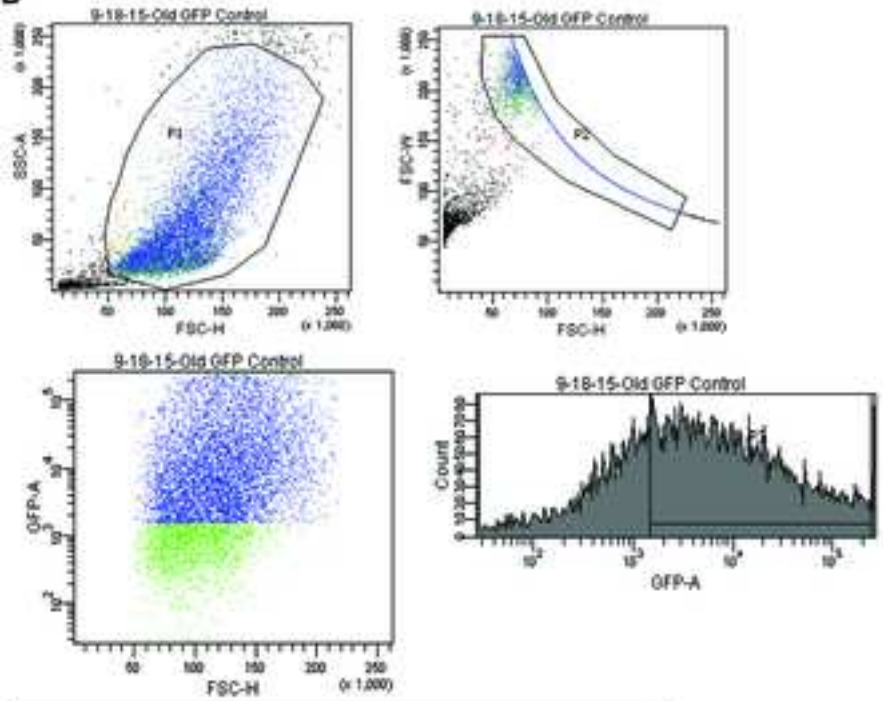

Tube: Old GFP Control

Population	#Events	%Parent	%Total
All Events	10,000	####	100.0
P1	8,441	84.4	84.4
P2	8,366	99.1	83.7
P3	6,182	73.9	61.8